약학박사학위논문

감염에 대한 초기 면역 방어 시스템에서 Tryptophanyl-tRNA Synthetase 의 역할 규명

Studies on the Role of Tryptophanyl-tRNA Synthetase in Early Defense against Pathogenic Infection

2017 년 2 월

서울대학교 약학대학원

약학과 의약생명과학전공

안 영 하

Contents

Studies on the Role of Tryptophanyl-tRNA Synthetase

in Early Defense against Pathogenic Infection

List of figures and tables

Studies on the Role of Tryptophanyl-tRNA Synthetase in Early Defense against Pathogenic Infection

Studies on the Role of Tryptophanyl-tRNA Synthetase

In Early Defense against Pathogenic Infection

감염에 대한 초기 면역 방어 시스템에서 Tryptophanyl-tRNA Synthetase 의 역할 규명

Running title: Secreted WRS as a primary defense system against infection

Keywords: secreted full-length tryptophanyl-tRNA synthetase (FL-WRS), sepsis, infection, innate immunity, endogenous ligand, TLR4

Abbreviations list

ARS: Aminoacyl-tRNA synthetase

WRS: Tryptophanyl-tRNA synthetase

WCL: Whole cell lysate

SUP: Supernant

TLR4: Toll like receptor 4

MD2: Myeloid differentiation factor 2

SIRS: Systemic inflammatory response syndrome

ASA: Asthma

RA: Rheumatoid arthritis

SS: Sjogren’s syndrome

Abstract

Tryptophanyl-tRNA synthetase (WRS) is a member of aminoacyl-tRNA synthetases (ARSs) and is an essential enzyme in protein synthesis. Recently, it is well known that these ARSs exhibit various biological functions in addition to their essential functions. Mini-WRSs lacking an extra N-terminal domain have been shown to inhibit angiogenesis. However, the secretion and function of the full-length WRS (FL-WRS) remain unknown. Here I report that the FL-WRS, but not mini-WRS, is rapidly secreted upon pathogen infection to prime innate immunity. Blood levels of FL-WRS were increased in the sepsis patients compared with healthy subjects, but not in those with sterile inflammation.

FL-WRS, which was present in cytoplasm of human monocytes, was secreted in a few minutes when pathogenic infectious agents (bacteria, viruses, fungi, etc.) invaded. The secreted FL-WRS, in combination with the TLR4-MD2 complex, increased the phagocytosis of macrophages and, at the same time, induces

neutrophil infiltration through chemokine secretion, thereby eradicating the infectious agent initially. The N-terminal 154 amino acid eukaryote-specific peptide of WRS was sufficient to recapitulate FL-WRS activity and its interaction mode with TLR4-MD2 is suggested.

Administration of FL-WRS into *Salmonella typhimurium*–infected mice reduced the bacteria counts in tissues and improved mouse survival, whereas its titration with the specific antibody aggravated the infection. These results suggest that FL-WRS acts as an early defense system to prevent pathogens from infesting at the initial stage of infection.

Introduction

Sepsis, or the invasion of microbial pathogens, is characterized by an overwhelming systemic inflammatory reaction, which can lead to severe sepsis and septic shock(van der Poll and Opal, 2008). During microbial infection, prompt and efficient innate inflammatory response is required for the elimination of microbial in host cells. Firstly, defensins and lysozymes directly kill microorganisms and digest bacterial cell walls. However, avoidance strategies of pathogens and multiplication of the pathogen to sufficient numbers overwhelm the immediate innate host defense. After entering tissues, innate immune cells sense the presence of pathogens via the interaction of pathogen-associated molecular

patterns (PAMPs) from invading pathogens with pattern recognition receptors (PRRs) such as Toll-like receptors (TLRs)(Dziarski and Gupta, 2000). TLR2 and TLR4 are surface expressed PRRs that recognize microbial lipopeptides and lipopolysaccharide (LPS), respectively (Takeuchi et al., 1999). For ligand recognition, TLR4 forms a homodimer (Park et al., 2009), whereas TLR2 forms a heterodimer with other TLRs such as TLR1 or TLR6. Normally, the extracellular domain of TLR4 forms a stable heterodimer with myeloid differentiation factor 2 (MD2), and dimerization of the TLR4-MD2 complex occurs in the presence of LPS that is delivered to MD2 (Park et al., 2009). As a consequence of endocytosis of the receptor-ligand complex, multiple signaling components are activated, including NF-κB. Ultimately activation of these signaling pathways lead to the productions of cytokines and chemokines, and recruitment

of innate inflammatory cells, such as neutrophils and monocytes/macrophages, which eliminate pathogens by phagocytosis (Fitzgerald et al., 2001).

Although many exogenous ligands capable of triggering innate immunity have been reported, the existence of endogenous molecules that specifically mediate pathogen infection in humans has only been suggested. For instance, chromatin-associated protein high-mobility group box 1 (HMGB-1), a highly conserved DNA binding protein, is known to be secreted by infection and to interact with TLR2 and TLR4. However, HMGB-1 does not appear to function rapidly at the frontline of infection, but rather at a relatively late phase, in the range of 8-12 hr after pathogen exposure (Wang et al., 1999). These data suggest that HMGB-1 expression is induced by TNF-α and IL-1β from immune cells exposed to PAMPs. Moreover, in an animal model of sepsis, serum level of

HMGB-1 increased over 18-72 hr period after infection and negatively affected survival (Yang et al., 2004). Heat shock protein 70 (HSP70) has been also suggested as a putative endogenous ligand for TLR4 (Vabulas et al., 2002), but it is not yet known whether the HSP70 secretion is associated only with infection. An important effect of the interaction between pathogens and tissue macrophages is activation of macrophages to release cytokines that bring phagocytes (monocytes, neutrophils and macrophages) to efficiently eliminate the microorganism invasion(Brown and Treacher, 2006; Chaplin, 2010). There are a number of mechanisms in which biologically active cytokine concentrations reach the relevant target cells, where the level and duration of cytokine synthesis do not result in inadequate activation of the immune and immune system(Kelso, 1998).

Aminoacyl-tRNA synthetases (ARSs) play an essential role in catalyzing the esterification reactions that link amino acids with cognate tRNAs for protein synthesis. Some ARSs are secreted by cells to undertake extracellular, non-canonical functions even under conditions that may interfere with their canonical mission (Son et al., 2014). Tryptophanyl-tRNA synthetase (WRS) freely exists in two forms in the cytoplasm: one as a full-length (FL) form and the other as a truncated form. The major truncated version, namely mini-WRS, is an alternatively spliced gene product with a key absence of its NH_2-terminal domain (a.a.1–47). Human FL-WRS has the unique NH_2-terminal eukaryotic extension domain (a.a.1–154), which is absent from prokaryotic WRS. Immune stimuli like IFN-γ potently induce WRS expression in higher eukaryote cells (Kisselev et al.,

1993; Shen et al., 1996). It is known that infection conditions such as intracellular pathogenic parasites, Vibrio cholera, Cytomegalovirus (CMV) and H3N2 swine influenza virus highly increased WRS expression level as well (Ellis et al., 2015) (Wu et al., 2013; Zhu et al., 1998). The development of eukaryotic specific extension domain of WRS assumed to contribute to immune function during infection. However, the functional activity of FL-WRS has not been reported and the only cleavage form of WRS has a potent anti-angiogenic effect (Wakasugi et al., 2002). In this study, I demonstrated that FL-WRS is actively secreted endogenous protein upon bacterial infection and amplified the infection signaling via activation of macrophages, leading to the recruitment of phagocytes.

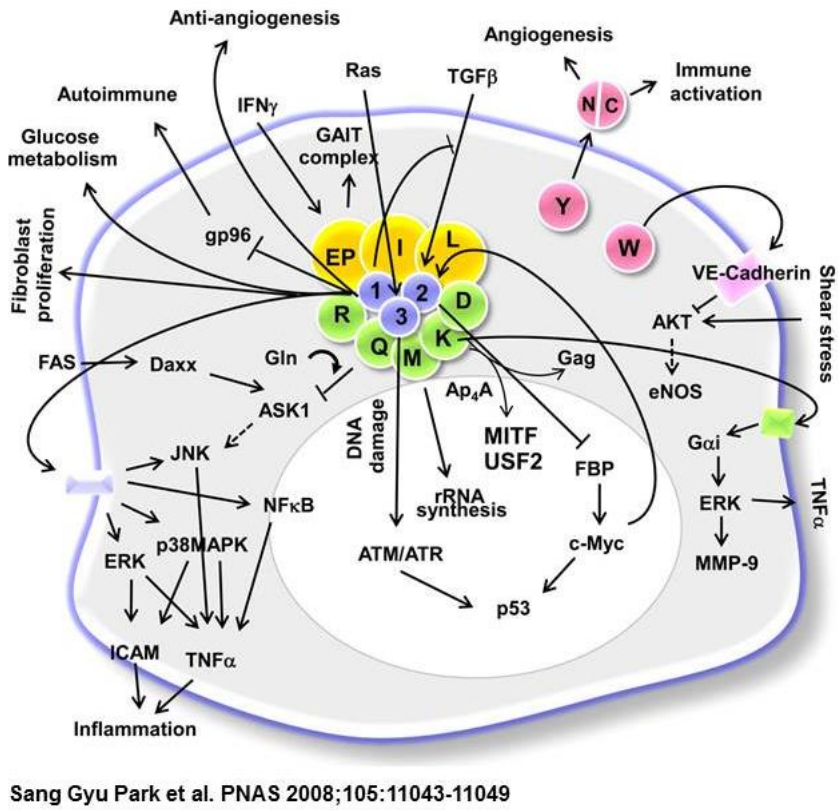

Sang Gyu Park et al. PNAS 2008;105:11043-11049

Signaling network mediated by mammalian aminoacyl tRNA synthetases (AARSs) Nine different AARSs (EP: glutamyl-prolyl-, I: isoleucyl-, L: leucyl-, M: methionyl-, Q: glutaminyl-, R: arginyl-, K: lysyl-, and D: aspartyl-tRNA synthetase) form a macromolecular complex with three nonenzymatic factors, AIMP1/p43, AIMP2/p38 and AIMP3/p18. Among noncomplex forming AARSs, WRS (tryptophanyl-tRNA synthetase) is secreted and its N-terminal truncation results in the formation of an active angiostatic cytokine that works via VE-

cadherin (Wakasugi et al., 2002)

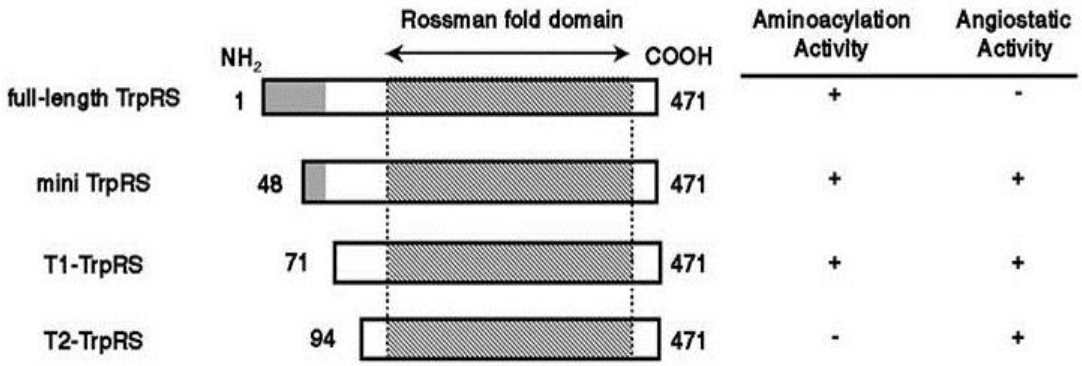

Atsushi Otani et al. PNAS 2002;99:178-183

Schematic representation of human WRS variants. Shaded regions of WRS represent the NH2-terminal appended domain. Numbers on the left and right correspond to the NH2- and COOH-terminal residues relative to the human full-length enzyme, respectively. WRS variants active (+) or inactive (−) in aminoacylation or angiogenesis inhibition assays are indicated. The NH2 domain of WRS has sequence similarity to the extra domains of human GluProRS (a fusion of glutamyl- and prolyl-tRNA synthetases), MetRS, GlyRS, and HisRS (Frolova et al., 1991; Ge et al., 1994; Hirakata et al., 1996).

Results

Chapter I. WRS is Secreted from Monocytes by Pathogenic Infection

Increase of WRS Serum Levels in Sepsis Patients

WRS is a constitutively expressed cytosolic protein and plays important intracellular roles. Current evidence indicates that WRS is released into extracellular serum and involves immune regulation (Bao et al., 2013). To examine whether WRS secretion into blood correlates with infection, I measured serum levels of WRS in sepsis patients with systemic infection. Compared with healthy controls (n=20, 0.18 ± 0.06 ng/mL), the levels of WRS increased about 27-fold in the sepsis patients with bacterial infection (n=100, 5.0 ± 0.63 ng/mL, $p<0.0001$) (Figure I-1a and Table 1). In contrast, there were no differences in the levels of glycyl-tRNA synthetase (GRS) (Figure I-1b). Although lysyl-tRNA synthetase (KRS) appeared to show higher mean value in sepsis patients than in

healthy controls, the difference was statistically not as significant as WRS (Figure I-1c) and additional analysis with more individuals seems to be necessary to reach convincing conclusion. Levels of WRS, but not GRS and KRS, also increased in fungal sepsis patients (n=8, 4.52 ± 1.83 ng/mL, $p<0.01$) (Figure I-1d, e, f, and Table 1). I did not observe significantly different levels of WRS between the patients infected with Gram-negative (n=62, 5.98 ± 0.93 ng/mL), Gram-positive bacteria (n=25, 2.87 ± 0.72 ng/mL), and fungi (n=8, 4.52 ± 1.83 ng/mL), or between those with multiple (n=11, 3.53 ± 1.22 ng/mL) and single pathogen infection (n=94, 5.01 ± 0.67 ng/mL, $p>0.05$) (Figure I-1g and 1h). To test whether WRS serum levels are increased in inflammatory immune disorders unrelated to infections, I measured WRS levels in sterile inflammatory disorders including systemic inflammatory response syndrome (SIRS), asthma patients (ASA), autoimmune disease patients diagnosed with rheumatoid arthritis (RA) and Sjogren's syndrome (SS), and found little difference between patients and healthy

controls (Figure I-1i, j, k). These data suggest that systemic infections would induce secretion of WRS into blood.

WRS-Specific Secretion by Pathogen Infection

To confirm that infection would induce the secretion of WRS, I measured the levels of WRS secreted from cultured human peripheral blood mononuclear cells (PBMCs) that were infected with various pathogens. Human PBMC were cultured for 2 hours at a density of 2×10^6 cells /mL and infected with 2×10^6 CFU of S. typhimurium (MOI = 1). Culture supernatants cultured for two hours after infection were precipitated with TCA and immunoblot experiments were performed on various kinds of ARS. Consistent with the data from sepsis patients, only WRS was detected in the culture medium among the tested ARSs including WRS, methionyl-tRNA synthetase (MRS), aspartyl-tRNA synthetase (DRS), GRS, histidyl-tRNA synthetase (HRS), KRS, and ARS-interacting multi-functional protein 1 (AIMP1). This shows that ARS secreted after bacterial infection is WRS

(Figure I-2a). Gram-negative bacteria such as *S. typhimurium* and *E. coli*, gram-positive bacteria such as *L. monocytogenes* and *S. aureus*, and *Candida albicans*, which is a fungus, also secrete WRS in human peripheral blood mononuclear cells (Figure I-2b). In addition, WRS secretion was induced by infection with respiratory cell virus (RSV) and PR8 influenza virus (Figure I-2c). This indicates that WRS responds to a variety of pathogens, not to certain bacteria. At this time, no significant secretion of HMGB1, HSP70 and lactate dehydrogenase (LDH) was observed (Figure I-2b and 2d). *In vivo* experiments using mice also confirmed the secretion of WRS by *S. typhimurium* infection. After intraperitoneal injection of *S. typhimurium* into the peritoneal cavity of mice, the amount of WRS was determined by mouse WRS ELISA. The secretion levels of WRS were dependent on the CFU of *S. typhimurium*. 1X10^8 CFU *S. typhimurium* -infected mice began to die from 8 hours, so WRS secretion was observed only up to 4 hours (Figure I-2e). Finally, I determined whether the release of WRS was from first-responder cells against bacterial infection. Monocytes patrol the blood vessel lumen by

associating with the vascular endothelium and sense the bacterial and viral component (Murray and Wynn, 2011; Shi and Pamer, 2011). B cells, T cells, NK cells and monocytes were isolated from PBMC with a commercial MACS depletion kits and infected with *S.typhimurium* for 2hrs. Among these immune cells, only monocytes released WRS following *S.typhimurium* bacterial infection (Figure I-2f). These data suggest that sensing of infection by patrolling monocytes promptly and actively release WRS.

Prompt Secretion of WRS Prior to TNF-α upon Infection

Many DAMPs (Damage-Associated Molecular Pattern molecules) are nuclear or cytoplasmic molecules and released outside the cell upon infection or tissue injury. DAMPs, including high mobility group box 1 protein (HMGB-1) and heat-shock proteins (HSPs) are passively released by necrotic cells or actively secreted in the late time by activated cells. In contrast to HMGB1 and HSP70, WRS was released

actively in the early time following bacterial infection. To investigate the importance of the immediate release of WRS at the early time, kinetics of the secretion of both WRS and TNF-α were analyzed by western blot and WRS ELISA method. TNF-α is one of the most important pro-inflammatory cytokines initiating innate inflammatory responses following bacterial infection; hence, I compared its kinetics to that of WRS. The presence of FL-WRS was apparent from 15 min following *S.typhimurium* infection and gradually increased in the supernatant, while secretions of mini-WRS were minimal. The levels of mature TNF-α in the supernatant were detectable at 120 min. (Figure I-3a and 3b). The levels of WRS mRNA were not changed up to 120min, indicating that preexisting WRS molecules were released immediately upon bacterial infection without induction of gene expression. Whereas mRNA level of TNF-α was increased at 30min and high expression levels were apparent at 120 min (Figure I-3c). I further investigated the secretion of WRS and TNF-α at late time after *S.typhimurium* infection. The WRS transcription was induced from 8 hr after infection to restore

normal intracellular WRS level within 24 hr. In contrast, TNF-α mRNA synthesis reached its peak levels in 2 hr after infection and then decreased (Figure I-3d and 3e)

Endocytosis of Pathogenic Components Affects WRS Secretion

I have determined whether WRS is secreted by TLR ligands or by inflammatory stimulus. Treatment of PBMC with LPS, Pam3CSK4, CpG oligonucleotides (ODN) and Zymosan resulted in dose-dependent WRS secretion. In contrast, other stimulus such as the inflammatory elements including TNF-α, liposomes or PS particles did not induce WRS secretion for up to 2 hours (Figure I-4a). I monitored the effect of endocytosis inhibitors such as dynasore and cytochalasin D to determine if the endocytosis of pathogens is required for WRS secretion. Endocytosis inhibitors were pretreated 30 minutes and found that the inhibitor-treated cells lost the WRS secretion activity (Figure I-4b). These results suggest that endocytosis of pathogen or pathogenic components, but not inflammatory

stimuli, would be required for the WRS secretion. In summary, FL-WRS appears to be secreted specifically from mononuclear cells in response to the endocytosis of the pathogen, and this event occurs prior to the activation of previously known innate immunity.

Chapter II. FL-WRS, but not Mini-WRS Activates Macrophages to Prime Innate Immune Responses

FL-WRS, but not Mini-WRS, Induces Cytokine/Chemokine Productions

Since amplification of innate immunity depends on the productions of chemokines and the recruitments of inflammatory cells, particularly neutrophils and macrophages. Therefore, I screened whether FL-WRS would induce chemokine and cytokine production in human PBMCs using microarray. FL-WRS induces innate inflammatory responses through macrophage activation, whereas mini-WRS has no relevance to immune activation. To investigate the type of

cytokine/chemokine secreted by FL-WRS, human PBMC were treated with FL-WRS or mini-WRS and then subjected to microarray. The mean pixel of TNF-α, MIP1-α, MIP1- IL-6 and IL-8 were highly increased compared with control (Figure II-1a). In addition, human monocytes were treated with FL-WRS or mini-WRS and cultured for 3 hours. The amount of TNF-α, MIP1-α and MIP1-β protein present in the culture supernatant was measured by ELISA Kit (San Jose, CA, USA and R & D systems). FL-WRS not only secreted TNF-α, MIP1-α and MIP1-β proteins by activating human PBMCs, but also increased mRNA expression levels. On the other hand, mini-WRS had no effect on cytokine secretion (Figure II-1b and 1c).

To investigate the type of immune cells responding to FL-WRS, FL-WRS was treated on various immune cells and the relative fold change of the secreted TNF-α and MIP1-α were determined. Mouse primary T cells, neutrophils, natural killer cells (Zhu et al.), monocytes and macrophages were prepared using a mouse microbead isolation kit (Miltenyi, Bergisch Gladbach, Germany). The

obtained cells showed more than 95% purity when analyzed by flow cytometry. The primary immune cells were cultured for 18 hrs after treatment with FL-WRS (100 nM), mini-WRS (100 nM) or LPS (100 ng / ml) according to the experimental conditions and the amounts of TNF-α and MIP1-α proteins were measured by ELISA kit. As a result, LPS significantly induced TNF-α and MIP1-α secretion in most immune cells, whereas FL-WRS showed the greatest effect in monocytes and BMDM. Mini-WRS also had no effect on cytokine secretion (Figure II-1d). In order to eliminate the endotoxin contamination of FL-WRS protein purified from E. coli, FL-WRS treated with heat or trypsin had no effect on TNF-α secretion after BMDM treatment (data not shown). In addition, cytokine secretion by FL-WRS was not decreased by polymyxinB, whereas the positive control LPS significantly decreased cytokine secretion by polymyxinB treatment (Figure II-1e). I prepared recombinant FL-WRS and mini-WRS from HEK293T cells to avoid potential LPS contamination and observed that this

protein also induced chemokine secretion to a level similar to those induced by *E. coil*-expressed FL-WRS (Figure II-1f)

FL-WRS Increases the Infiltration of Phagocytes via Macrophage Activation

The effect of FL-WRS on the migration of immune cells was examined using a transwell migration assay (Figure II-2a). BMDMs were treated with FL-WRS or mini-WRS and cultured for 18 hours. The culture was transferred to a 24-well plate. Various primary immune cells were isolated from the mice and then placed in the upper part of the migration chamber and incubated at 37° C for 4 hours. As a result, it was observed that the culture supernatant of the FL-WRS treated-BMDM greatly increased monocyte, neutrophil and BMDM infiltration. In contrast, the FL-WRS protein itself (data not shown) or mini-WRS-treated culture supernatant had no effect on cell migration. To investigate the effect of FL-WRS on the innate immune response, *in vivo* imaging of neutrophil, monocyte/macrophages recruitment was monitored. Alexa647-labled FL-WRS or

mini-WRS was injected into transgenic mice overexpressing GFP-LysM, and the inflow of neutrophil, monocyte, macrophages exhibited by green fluorescence was photographed for up to 4 hours. As a result, mice injected with FL-WRS showed a marked increase in neutrophils infiltration compared to the control and mini-WRS injected mice (Figure II-2b). When mice were *i.p.* injected with FL-WRS, the numbers of $Ly6G^{+}$neutrophils, $CD11b^{+}$ myeloid cells, and $CD11b^{+}F4/80^{+}$ macrophages infiltrated into peritoneal exudate were increased 15-, 9-, and 2-fold, respectively, compared with those injected with mini-WRS and the PBS-treated control (Figure II-2c). To confirm whether the induction of innate immune response by FL-WRS is macrophage-dependent, liposomal clodronate was treated for 24 hours to produce macrophage-deficient mice. Splenocytes obtained from macrophage-deficient mice showed a decrease in secretion of TNF-α and MIP1-α by FL-WRS, as well as inhibition of intraperitoneal neutrophil infiltration in vivo (Figure II-2d and 2e).

FL-WRS Increases Phagocytosis via Macrophage Activation.

Matured or activated macrophages express high levels of CD80 (B7-1) or CD86 (B7-2) on the surface and interact with CD28 to provide a second signal to the T cell. Other molecules like CD40 serves as co-stimulator or amplifier of initial stimulatory signal to T-cell. I examined whether FL-WRS affects the expression of cell surface molecules in macrophages. BrdU cell proliferation experiments confirmed that cell proliferation was reduced when FL-WRS was treated to BMDM cells. Flow cytometry analysis using Cd11b and F4/80 at the top of Fig. 7b indicates that bone marrow cells were well differentiated into BMDM. The differentiated BMDMs were treated with FL-WRS or mini-WRS (100 nM) for 18 hours and CD40, CD80 and CD86 protein expression levels were measured by flow cytometry. These results indicate that BMDMs are matured by FL-WRS (Figure II-3a and 3b). To determine how FL-WRS functions in this rapid response to infection, I checked whether FL-WRS would affect the phagocytic activities *in vivo* and *in vitro*. Phagocytic cells were captured and counted using *in vivo*

imaging technology. The number of phagocytic cells was significantly increased in the FL-WRS-treated mice, compared to those in mini-WRS- and PBS-treated mice (Figure II-3c). I also examined the effect of FL-WRS on the phagocytosis of bone marrow-derived macrophage (BMDM) (Figure II-3d). BMDM was cultured in a 96-well culture dish overnight, then replaced with RPMI medium without M-CSF, and treated with FL-WRS or mini-WRS for 18 hours. After washing the cells, 100 μL of fluorescein-labeled E. coli bioparticles (Vybrant phagocytosis assay kit, Invitrogen) was added and incubated for 2 hours, after which the culture was removed and 100 μL of trypanblue for 1 min to inhibit autofluorescence. The fluorescence signal from the macrophage was measured at 485 (excitation) and 520 nm (emission) wavelengths and the phagocytosis index was calculated. The results showed that the FL-WRS-treated BMDM increased the phagocytic index more than 3-fold compared to the control group.

FL-WRS Protects Bacteria-Infected Mice from Lethality.

In order to investigate the effect of FL-WRS on in vivo bacterial infection inhibition, the survival rate of S. typhimurium-infected mice and S. typhimurium adhesion and uptake by infiltrated neutrophil were confirmed after infection. Fluorescence-labeled *S.typhimurium* (FITC-ST) was injected intraperitoneally into mice (C57BL / 6 mice, 9-12 week old female). Five minutes later, PBS or mouse FL-WRS (mFL-WRS) or mouse ΔN51-WRS (mΔN51-WRS) protein was injected. Two hours after infection, mice were sacrificed and the cells in the peritoneal cavity were separated, stained with Ly6G antibody, and analyzed for flow cytometry. As a result, the number of uptake of S. typhimurium by infiltrating neutrophils (FITC-*S. typhimurium*$^{+}$ Ly6G $^{+}$ neutrophil) was significantly increased in the mFL-WRS treated group compared to the PBS-treated control group (Figure II-4b). Animal experiments with mice were carried out according to the outline of experiment (Figure II-4a) and the degree of bacterial clearance in the spleen and liver was observed 4 hours after infection. Four hours after infection with *S. typhimurim*, spleen and liver homogenate were

serially diluted and spotted on NB agar medium. After culturing at 37 ℃ for 24 hours, the bacterial CFU was calculated and analyzed. As a result, it was confirmed that bacterial CFU in the spleen and liver was significantly decreased in the mFL-WRS treated group. Immunohistochemistry also confirmed that the number of bacteria in the spleen and liver decreased (Figure II-4c and 4d). This shows that in the spleen of FL-WRS-treated mice, bacteria were eliminated before they caused cell infections. To investigate the effect of mFL-WRS on the survival rate of *S. typhimurium*-infected mice, animal experiments using mice were performed according to the outline of the experiment and survival analysis was performed. mice were injected with PBS, mFL-WRS, or mΔN51-WRS at 5 minutes after intraperitoneal injection of 1X107 CFU S. typhimurium. Survival rates of 24, 48, 72, and 96 hours after infection were expressed as survival plots according to treatment conditions. As a result, the survival time of mFL-WRS injected group was significantly longer than that of control group or mΔN51-WRS group (Figure II-4e).

In addition to S. typhimurium, a gram-negative strain, *L. monocytogenes*-infected mice also showed decreased numbers of bacteria in the spleen and liver and increased survival in the mFL-WRS-treated group (Data not shown). These results show that FL-WRS reduces the mortality rate of bacterial infected mice by activating innate immune responses early in infection

Neutralization of FL-WRS Aggravates Bacterial Infection

In order to further validate the role of FL-WRS as an initial immune defense *in vivo* infection, scFv antibodies neutralizing the function of FL-WRS were constructed. A 4G1 scFv that specifically binds to the N154 peptide of human WRS was selected by panning a library of human single chain variable fragments (scFv) expressed in phage (Figure II-5a). The 4G1 scFv clone binds to the FL-WRS protein but does not bind to the mini-WRS protein. In addition, when FL-WRS and 4G1 were simultaneously treated with PMA-differentiated THP-1 cells, the amount of TNF-α secreted by FL-WRS was significantly decreased. On the

other hand, the GRS scFv antibody used as a negative control did not affect the amount of TNF-α secreted by FL-WRS (Figure II-5b and 5c). When *S. typhimurium* was injected into the abdominal cavity simultaneously with scFv 4G1 or scFv 2B (bound to GRS), the production of TNF-α and MIP-1α was significantly reduced in scFv 4G1-treated mice. In addition, intraperitoneal neutrophil infiltration was reduced and survival rate was decreased in scFv 4G1 treated mice. The scFv 2B-treated mice used as negative controls did not significantly affect cytokine, neutrophil infiltration, and survival rates (Figure II-5d, e, f). All these results further demonstrate the importance of FL-WRS in vivo in the early immune defense system.

Chapter III. FL-WRS Activates Innate Immunity via Dimerization with TLR4-MD2 Complexes

Mechanism of Innate Immune Activation by FL-WRS via TLR4-MD2

To understand molecular mechanism of FL-WRS, I screened whether FL-WRS acts as a ligand for innate immune receptors to induce early immune activation. Figure III-1a shows experimental results using the NF-kB luciferase reporter system. HEK293 cells expressing PRR such as NF-kB reporter, toll-like receptor (TLR), NOD-like receptor (NLR) and C-type lectin receptor (CLR) were stimulated with FL-WRS for 16-20 hours (Relative activity, (%)). Experimental results showed that FL-WRS acts as a ligand for TLR2 and TLR4/MD2 (myeloid differentiation factor 2) receptors. I examined the ability of FL-WRS to activate NF-kB signaling in immune cells and examined the pattern-recognition receptor (PRR) associated with the immune activation of WRS. In the FL-WRS-treated macrophages, the levels of NF-κ B p65 in the nucleus, cytoplasmic phosphorylated IκB-α (p-IκB-α) and phosphorylated ERK (p-ERK) level were significantly increased in a dose-dependent manner. In contrast, mini-WRS-treated macrophages did not phosphorylate NF-kB signaling proteins (Figure III-

1b). Experiments were conducted to confirm the effect of TLR receptor and MD2 expression on the secretion of cytokines in BMDM. BMDM were transfected with siRNA for each TLR and MD2 for 48hrs, and then treated with FL-WRS for 18 hours and levels of TNF-α and MIP-1α secreted from BMDM were measured by ELISA method. The results showed that the FL-WRS-induced TNF-α and MIP-1 α productions were significantly inhibited when TLR4, MD2, and TLR2 (to lesser degree) were suppressed (Figure III-1c).

I examined the manner in which KO (knock-out) mice that do not express TLR2, TLR4, or MD2 respond to FL-WRS. BMDM derived from TLR2 KO, TLR4 KO, or MD2 KO mice showed a marked decrease in the amount of MIP-1α and TNF-α secreted in response to FL-WRS, compared with BMDM derived from wild-type (WT) mice (Figure III-1d). In addition, phagocytic activities in BMDMs were significantly suppressed in $TLR4^{-/-}$and $MD2^{-/-}$mice (Figure III-1e). The peritoneal exudate cells (PECs) were harvested 4 hours after intraperitoneal injection of FL-WRS (20 ug per mouse) into each KO mouse, and the infiltrated

neutrophils ($Ly6G^+$ Neutrophil) were significantly reduced than WT mice (Figure III-1f). Compared with TLR2 KO mice, TLR4 and MD2 KO mice showed almost complete inhibition of innate immune activation by FL-WRS, and TLR4 and MD2 expression inhibition effects were more pronounced than TLR2. While the *i.p.* injection of mFL-WRS after ST inoculation significantly diminished bacterial loads and improved survival rates in the $TLR4^{+/+}$ mice, these effects were not shown in $TLR4^{-/-}$ mice (data not shown). These results suggest that FL-WRS acts on the NF-kB signaling pathway in macrophages and innate immune activation is mediated by TLR4/MD2 receptor.

Direct Interaction of FL-WRS and TLR4-MD2

To understand the mechanism by which WRS activates TLR4-MD2, I examined whether WRS directly binds to TLR4-MD2. The direct binding of WRS to TLR4 and MD2 was confirmed by GST pull-down experiment (Figure III-2a). Pull-down of MD2 or TLR4 with GST-fused FL-WRS protein (GST/FL-WRS) or

GST-fused mini-WRS (GST/mini-WRS) increased the level of co-immunoprecipitated MD2 and TLR4-MD2. As a result, FL-WRS was co-immunoprecipitated with MD2, but not with TLR4. FL-WRS and MD2 are directly interacted but FL-WRS and TLR4 do not bind directly without MD2. Therefore, it shows the combination of FL-WRS and MD2 must precede binding to TLR4 to form a complex, Mini-WRS showed a decrease in the level of binding to MD2 compared with FL-WRS, but mini-WRS also showed a result of binding to MD2. On the other hand, both FL-WRS and mini-WRS did not bind to TLR4. To understand how FL-WRS would activate TLR4-MD2, I prepared a series of the N-terminal peptides (Figure III-2b) and compared their cytokine production activities. Among them, N154 showed the activity comparable to FL-WRS (Figure III-2c) and its activity showed the dependency on TLR2, TLR4, and MD2 (Figure III-2d), proving that N154 is sufficient to mediate the activity of FL-WRS.

The characteristics of the binding between WRS and TLR4-MD2 were studied in detail using surface plasmon resonance (SPR). Using SPR analysis, I confirmed

that FL-WRS and mini-WRS could bind to MD2 with Kd of 190 and 200 nM, respectively (Figure III-2e), while they showed no binding signal to TLR4 (Figure III-2f). I also checked binding of the different N-terminal fragments to MD2 and TLR4. Despite the fact that N65 containing WHEP domain and even its shorter fragment, N47, showed the binding to both of MD2 and TLR4, they did not induce the cytokine production (Figure III-2b), further suggesting that binding to TLR4 and MD2 is not sufficient to work as an active ligand. Interestingly, N115, N125, and N135 showed no binding to MD2 and TLR4 (Figure III-2g and 2h) even though they contain the WHEP domain. Perhaps, the peptide region beyond N65 could mask the WHEP domain for the interaction with MD2. However, the peptides longer than N135 (N154 and N145) partially restored the binding to TLR4, but not MD2, with the cytokine-inducing activity suggesting that the peptide region beyond N135 might have an additional binding site for TLR4 and that this region would be additionally required for the ligand activity.

Modeling Study of the Interaction of WRS and TLR4-MD2 Dimers

Based on the data above (Figure III-2) and previous modeling study of TLR4-MD2 dimerization by homodimeric radioprotective 105 (RP105)/MD1 complex (Yoon et al., 2011), I generated a binding model of WRS homodimer (Yang et al., 2003) with two TLR4-MD2 complexes using their respective crystal structures. The docking model suggested that the N-terminal WHEP domain (8-64 aa) of helix-turn-helix motif (marked red) (Figure III-3a) would be inserted into the interface between TLR4 and MD2, making interactions with both proteins (Figure III-3b). This could explain why N47 is critical for the activity of FL-WRS. Further, the model with two TLR4-MD2 complexes suggests additional region spanning 145-152 aa (shown in red) that might interact with TLR4 *in trans* (Figure III-3c). Thus, N154 would be able to bring two TLR4-MD2 units for functional dimerization (Figure III-3c and 3d).

To validate this model, I introduced mutations at the residues that were suggested to

make interactions with TLR4-MD2. Among them, the L10D mutation of FL-WRS almost completely ablated the cytokine production activity (Figure III-3e), further confirming the functional importance of N47 region. In addition, the N152G mutation also significantly reduced the cytokine-inducing activity, supporting the potential existence of the additional TLR4-binding site that would make an interaction with TLR4-MD2 *in trans*. Taken together; N154 would be fully active as a ligand, facilitating the dimerization of the two TLR4-MD2 units (Figure III-3f). However, the isolated WHEP domain (N65) can only bind one unit of TLR4-MD2 since it lacks the secondary TLR4-binding site that is present in N154. Although mini-WRS lacking N47 can bring the two TLR4-MD2 complexes into proximity through homodimerization of the WRS catalytic domain (Guo et al., 2010), they may not be able to induce the functional dimerization of TLR4-MD2 to activate the downstream signaling.

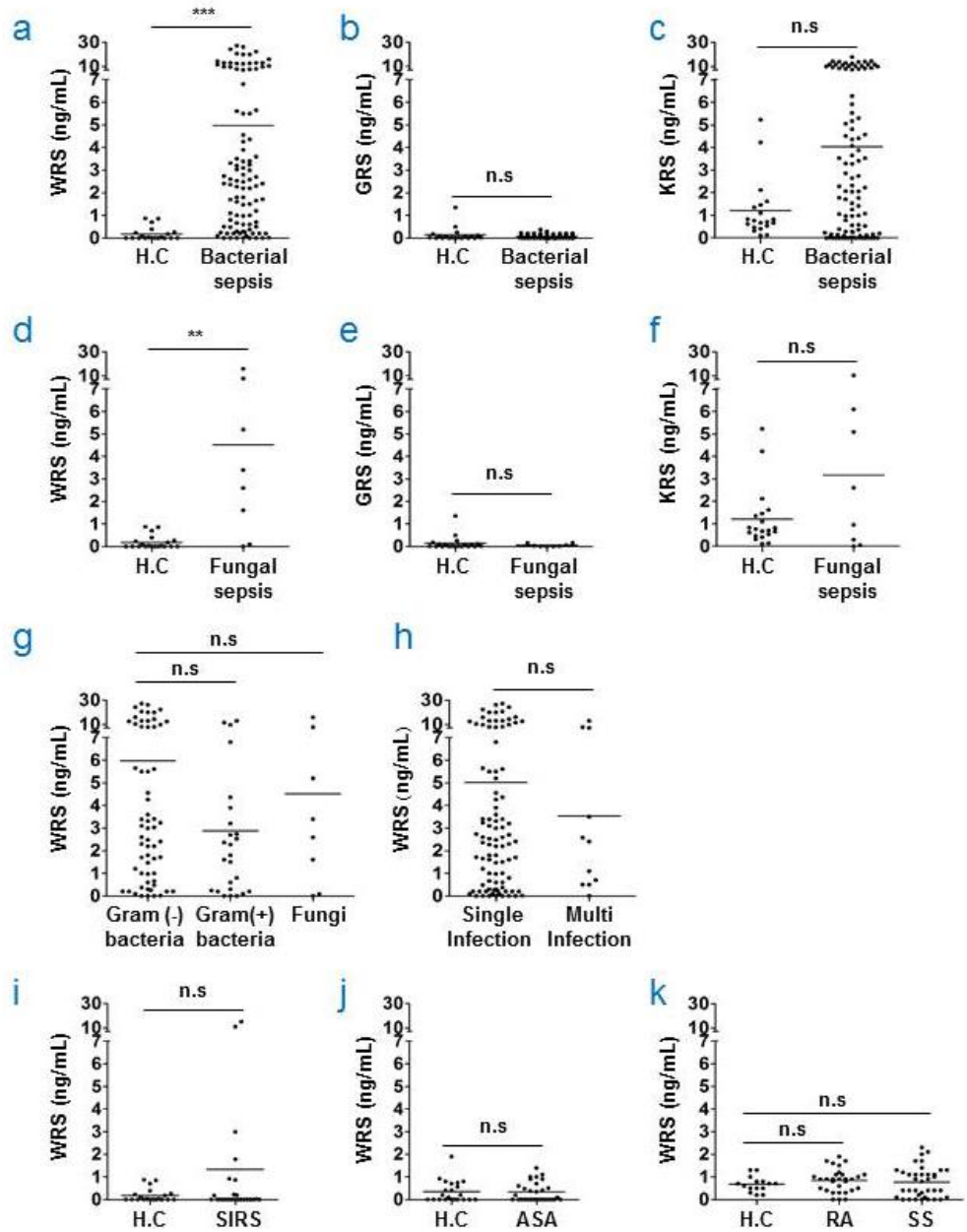

Figure I-1. Serum Levels of WRS in Patients with Sepsis and Sterile Inflammatory

Immune Disorders. Serum levels of (a) WRS, (b) GRS, and (c) KRS in healthy controls (n=20) and bacterial sepsis patients (n=100) were measured by ELISA specific for each ARS. Serum levels of **(d)** WRS, **(e)** GRS, and **(f)** KRS in healthy controls (n=20) and fungal sepsis patients (n=8) were measured by ELISA. Comparison of serum levels of WRS in sepsis patients infected with **(g)** Gram-negative (n=62), Gram-positive (n=25) bacteria, and fungi (n=8), and **(h)** with a single (n=94) or multiple (n=11) pathogens. Serum levels of WRS **(i)** in healthy control (n=20) and SIRS patients (n=25), **(j)** in healthy control (n=22) and ASA patients (n=30), and **(k)** in healthy control (n=15), RA (n=30), and SS (n=45) patients were measured by ELISA. All data are presented as scatter dot with mean of triplicate measurements. H.C; healthy control, n.s; not significant, **p<0.01, ***p<0.001, two-tailed Mann-Whitney test against healthy control.

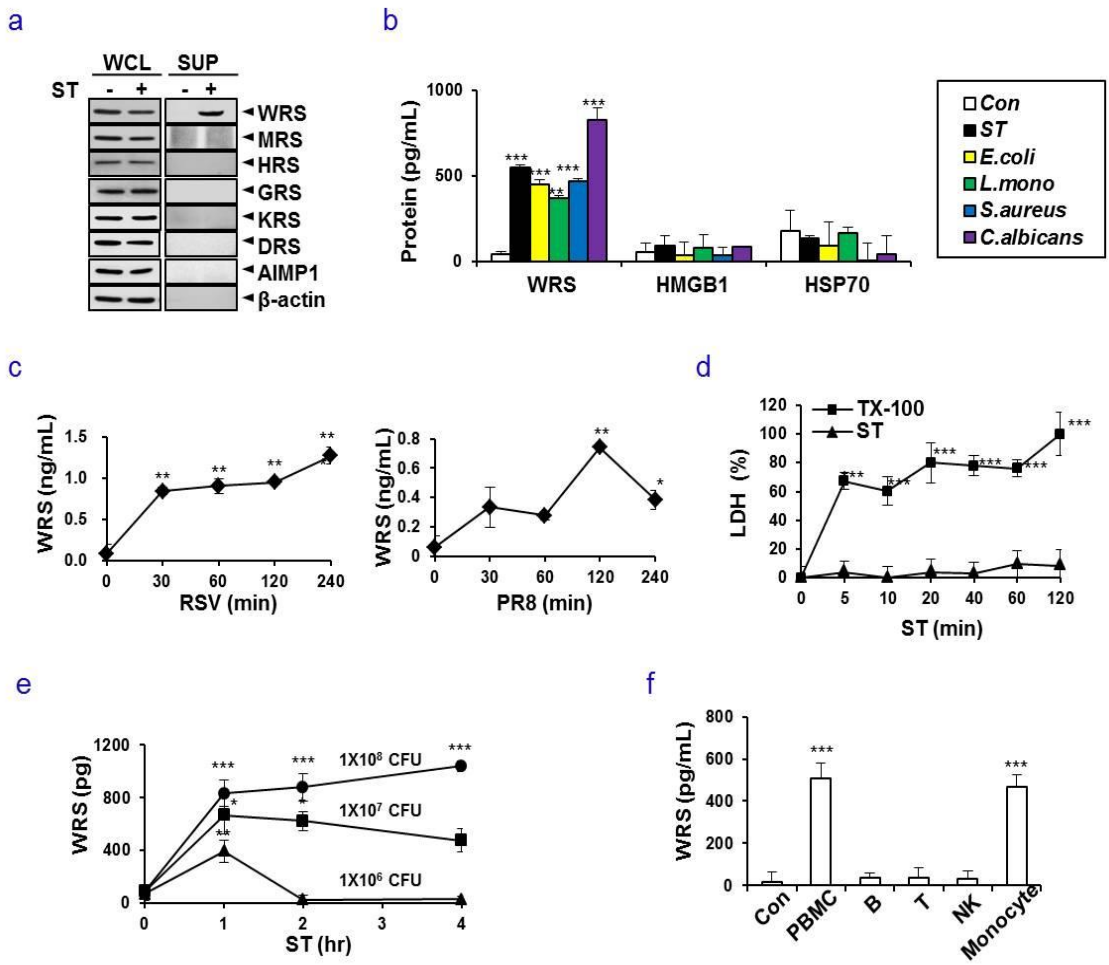

Figure I-2. Pathogenic infection induced the secretion of WRS. (a) The levels of ARSs in the supernatants (SUP) and whole cell lysates (WCL) of *Salmonella typhimurium* (ST)-infected human PBMCs (MOI=1) for 2 hr were detected by Western blot analysis. **(b)** The levels of WRS, HMGB-1, and HSP70 in the culture supernatants

of PBMCs following ST, *E. coli*, *L. monocytogenes*, *S. aureus*, and *C. albicans* (MOI=1) infection for 2 hr were measured by ELISA. **(c)** Secretion of WRS by virus infection. ELISA measurement of WRS in the cell culture supernatant of human PBMCs infected with respiratory syncytial virus (RSV) A2 or influenza A PR8 virus (both MOI=2) at the indicated time points. **(d)** The levels of LDH in ST-infected (MOI=1) or 1% TX-100-treated PBMCs were measured by LDH detection kit. **(e)** Mice were *i.p.* injected with indicated CFU of ST and the level of WRS in peritoneal lavage was measured by ELISA. Data are represented as mean ± SEM (n=5-11 for each time point). **(f)** The subsets of immune cells were isolated and infected with ST (MOI=1) for 2 hr. The levels of WRS in the cell culture supernatant were measured by ELISA. For panels b-f, the data are expressed as mean± SD of triplicate measurements. The statistical significance of the data (*$p<0.05$, **$p<0.01$, ***$p<0.001$) was determined against untreated control (b-f) (one-way ANOVA). For panels a, experiments were repeated three times.

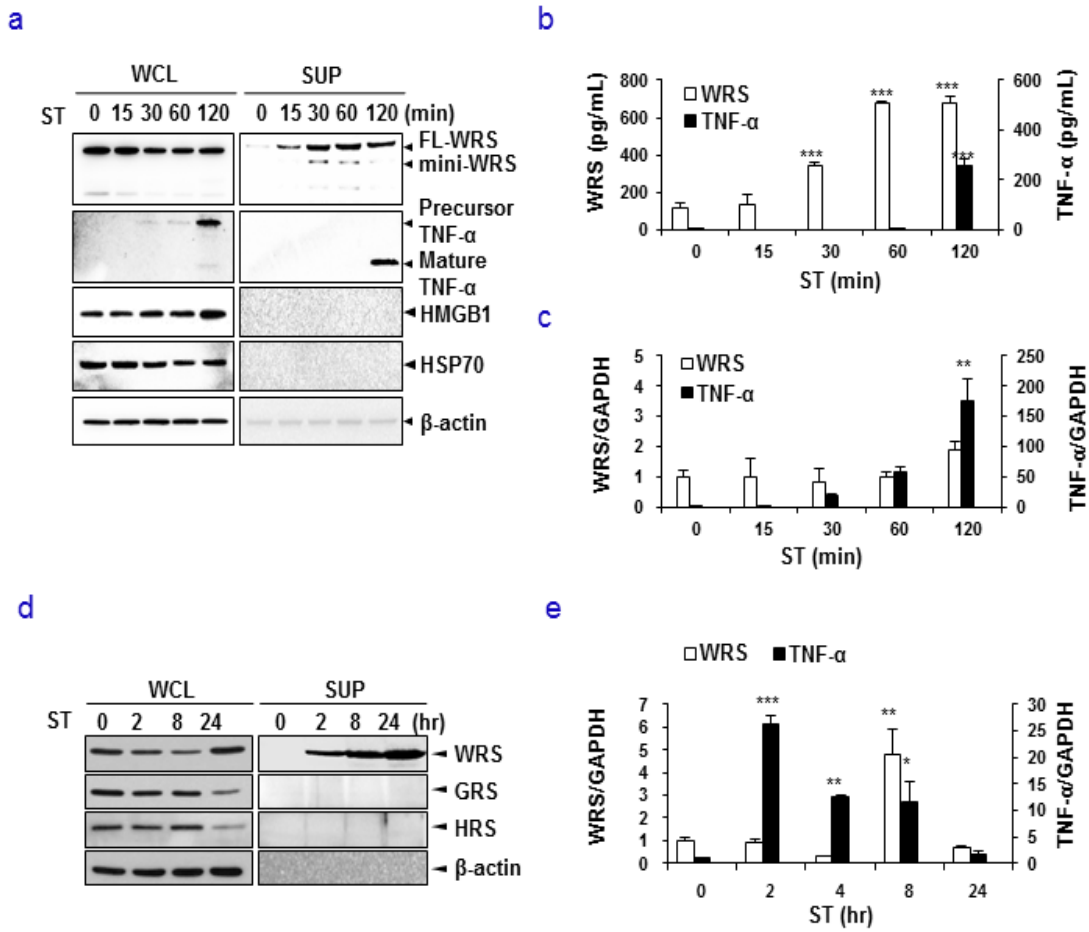

Figure I-3. WRS is promptly secreted prior to TNF-α upon Infection. (a) The levels of WRS, TNF-α, HMGB-1, HSP70, and β-actin in the supernant (SUP) and whole cell lysate (WCL) of ST-infected PBMCs (MOI=1) were detected by

Western blot analysis. **(b)** The levels of WRS and TNF-α in cell culture SUP of ST-infected PBMC were measured by ELISA. **(c)** The mRNA levels of WRS and TNF-α in PBMCs infected with ST (MOI=1) at indicated time points were determined by real time-PCR **(d)** WRS secretion and expression during extension of ST infection. Secretions of WRS, GRS, and HRS were analyzed in the culture supernatant (SUP) and whole cell lysates (WCL) of ST-infected PBMCs (MOI=1) by Western blot analysis using each specific antibody. **(e)** The mRNA expressions of WRS and TNF-α were analyzed by real-time PCR at the indicated time points. For panels b, c and e, the data are expressed as mean± SD of triplicate measurements. The statistical significance of the data (*$p<0.05$, **$p<0.01$, ***$p<0.001$) was determined against untreated control (b, c, e) (one-way ANOVA). For panels a and d, experiments were repeated three times.

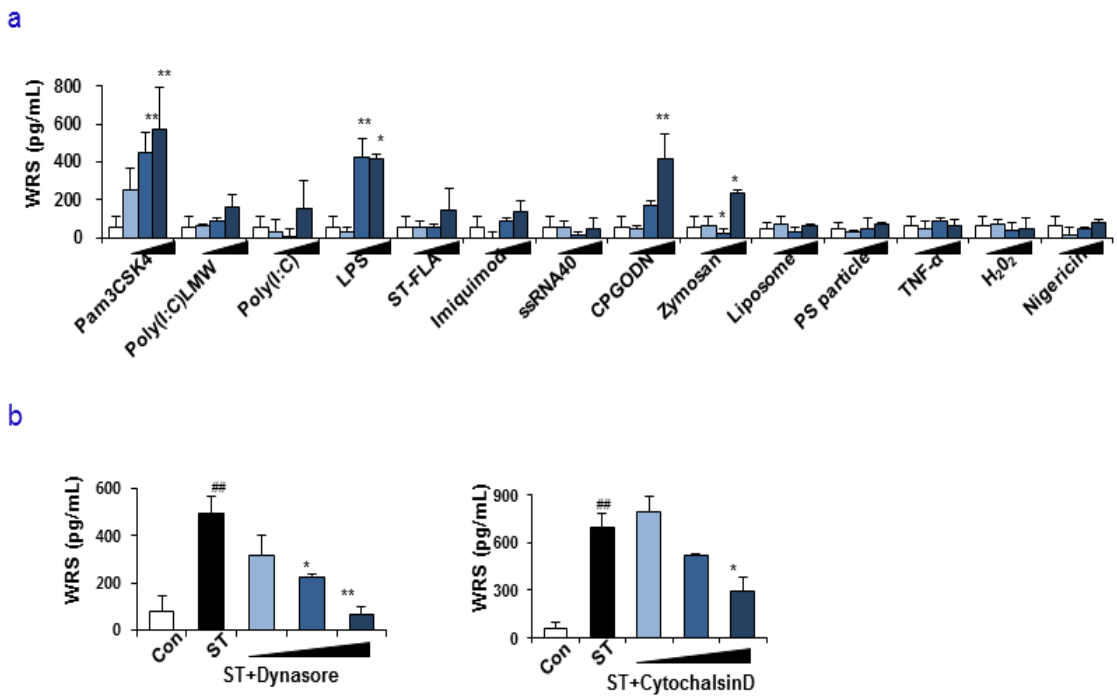

Figure I-4. Endocytosis of pathogenic components affects WRS secretion. (a)

The levels of WRS in the culture supernatants of PBMCs treated with increasing doses of Pam3CSK4, poly(I:C) LMW, poly(I:C), LPS (0.1-10 μg/mL), ST-FLA, imiquimod, ssRNA40, CPGODN (0.01-1 μg/mL), zymosan (0.1-10 μg/mL), liposome (0.005-0.5 mg/mL), PS particle (1:1-10 cell to bead ratio), TNF-α (0.01-

1 μg/mL), H_2O_2 (0.01-1 mM), and nigericin (10-250 μM) for 2 hr were measured by ELISA. **(b)** PBMCs were treated with dynasore (1-100 μM) or cytochalasin D (1-100 μM) for 30 min before ST infection, and the levels of WRS in the cell culture supernatant were measured by ELISA. The data are expressed as mean± SD of triplicate measurements. The statistical significance of the data (*$p<0.05$, **$p<0.01$, ***$p<0.001$) was determined against untreated control (a) or ST-infected control (b) (one-way ANOVA).

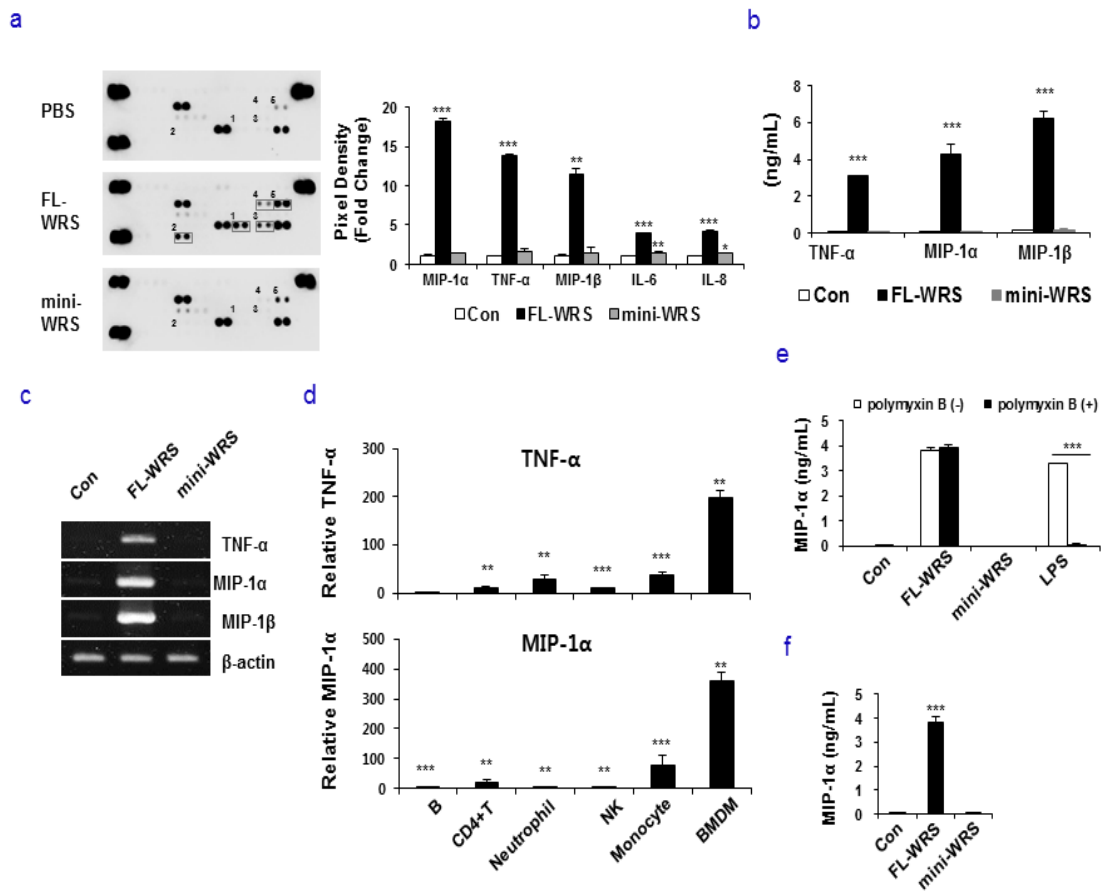

Figure II-1. FL-WRS, but not mini-WRS, Induces Cytokine and Chemokine

Productions (a) Protein array of cytokine/chemokine in culture supernatant of human PBMCs treated with PBS, FL-WRS (10 nM), and mini-WRS (100 nM) for 3 hr. The mean pixel densities of MIP-1α, TNF-α, MIP-1β, IL-6, and IL-8 were

analyzed using Image Lab 4.1 software. Experiments were performed in duplicate. PBMCs were treated with PBS, FL-WRS (10 nM), and mini-WRS (100 nM) for 3 hr and **(b)** the levels of TNF-α, MIP-1α and MIP-1 in the cell culture supernatant and **(c)** mRNA were determined by ELISA and RT-PCR, respectively. **(d)** Cultured mouse primary immune cells (B, CD4+T, neutrophil, NK, monocyte and BMDM) were treated with FL-WRS (100 nM) for 18 hr and levels of TNF-α and MIP-1α in the cell culture supernatants were measured by ELISA. The relative secretion was calculated by comparing with that of control. **(e)** ELISA measurement of MIP-1α in the cell culture supernatant of BMDMs treated with FL-WRS (100 nM), mini-WRS (100 nM), and LPS (100 ng/ml) in the presence or absence of polymyxin B (50 μg/mL) for 18 hr. **(f)** ELISA measurement of MIP-1α in the culture supernatant of BMDMs treated with recombinant FL-WRS and

mini-WRS (100 nM) isolated from HEK293T cells. For panels a, b, d, e and f, the data are expressed as mean± SD of triplicate measurements. The statistical significance of the data (*p<0.05, **p<0.01, ***p<0.001) was determined against untreated control (one-way ANOVA). For panels c, experiments were repeated three times.

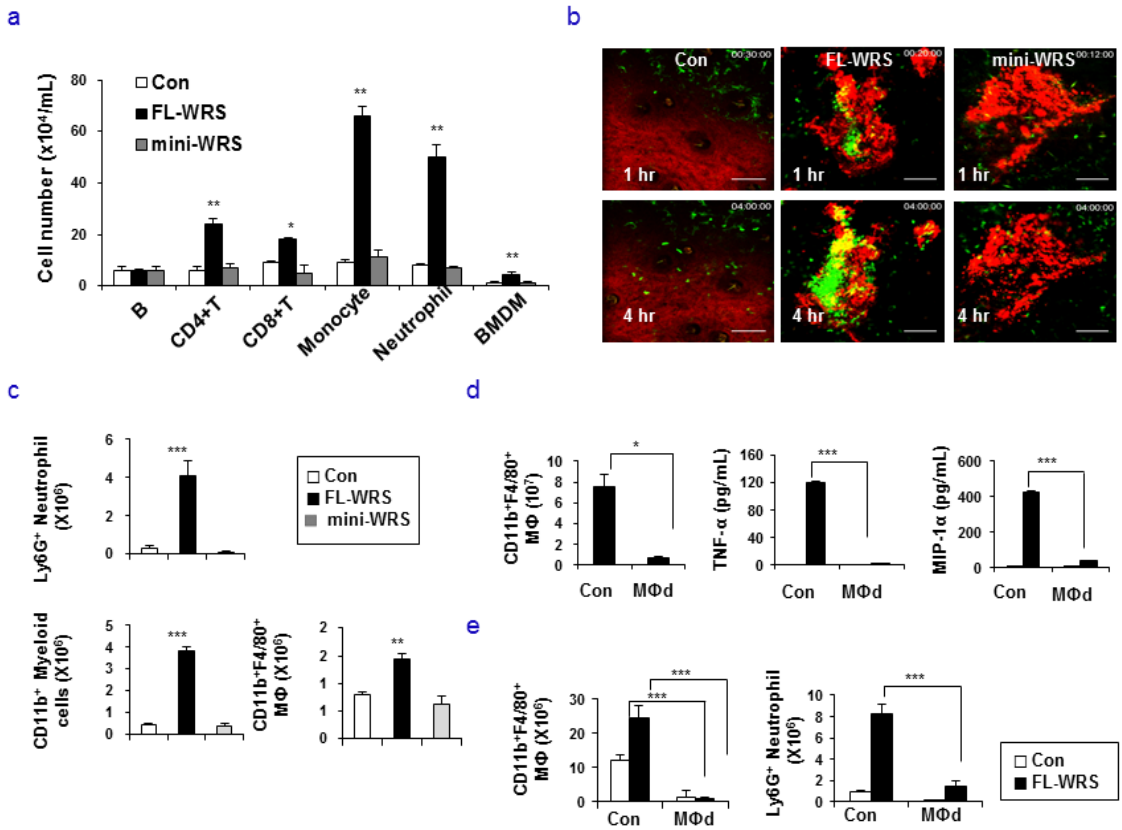

Figure II-2. FL-WRS increased the infiltration of phagocytes via macrophage activation. (a) Transwell migration assay. The number of migrated primary immune cells toward culture supernatants of FL-WRS-treated BMDMs was counted. **(b)** The infiltration of GFP-labelled neutrophils, monocytes and macrophages by FL-WRS, mini-WRS or PBS were monitored in GFP-lysM

transgenic mice using *in vivo* imaging system. **(c)** Mice were *i.p.* injected with PBS, FL-WRS and mini-WRS (each 20 μg/mouse) for 4 hr and the number of PECs was analyzed by flow cytometry. **(d)** Splenocytes from macrophage-depleted mice (MΦd) were treated with FL-WRS (100 nM) for 18 hr, and the levels of TNF-α and MIP-1α were measured by ELISA. The number of $CD11b^{+}F4/80^{+}$ cells in splenocytes was analyzed by flow cytometry. **(e)** Macrophage-depleted mice were *i.p.* injected with FL-WRS (20 μg/mouse) for 4 hr and the numbers of $CD11b^{+}F4/80^{+}$ and $Ly6G^{+}$ cells in PECs were analyzed by flow cytometry. For panels a and d, data are represented as mean ± SD of triplicate measurements. For panels c and e, experiments are repeated two times independently and data are represented as mean ± SEM (n=10). The statistical significance of the data against each control was represented as $*p<0.05$, $**p<0.01$, $***p<0.001$ (one-way ANOVA). For panels b, experiments were repeated three times.

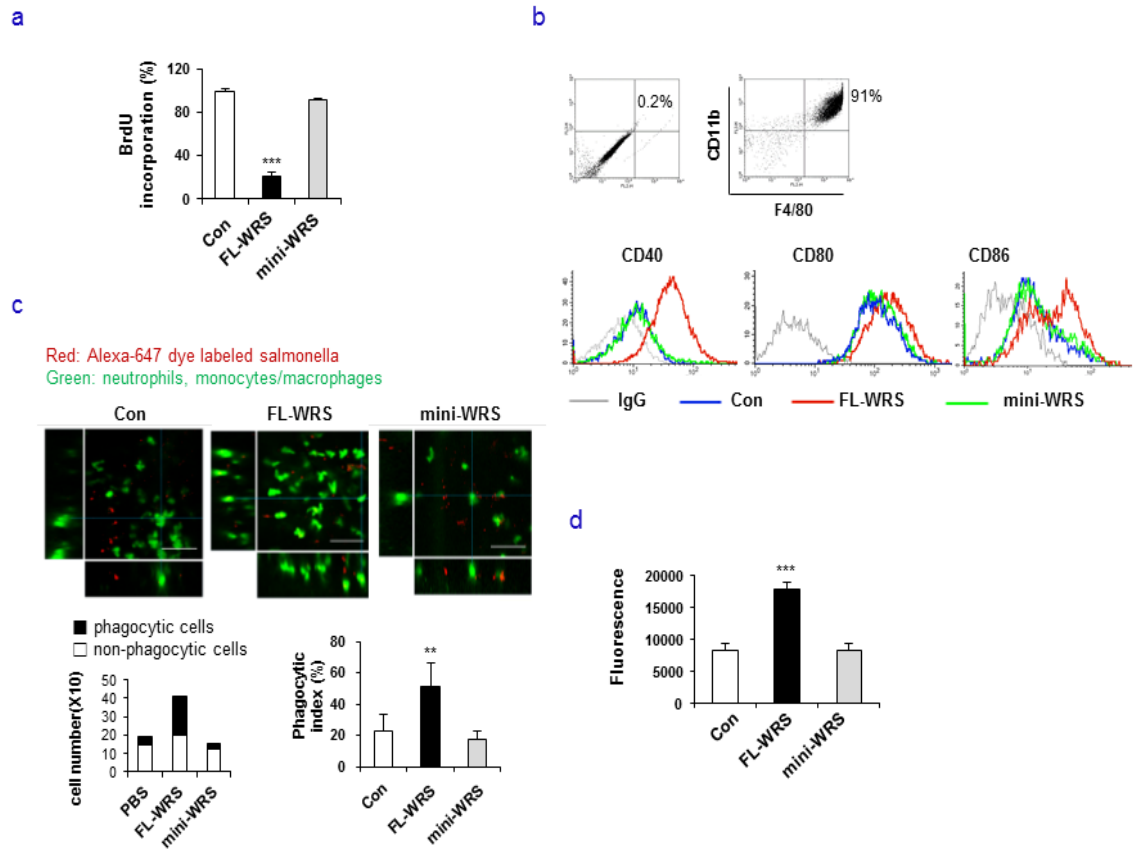

Figure II-3. FL-WRS increase phagocytosis via macrophage activation. **(a)** BMDMs were treated with PBS, FL-WRS (100 nM), and mini-WRS (100 nM) for 18 hr. The incorporation of BrdU was detected using BrdU cell proliferation assay kit, purchased from Cell Signaling. **(b)** Cell surface expressions of CD40, CD80

and CD86 in BMDMs treated with PBS, FL-WRS (100 nM), and mini-WRS (100 nM) for 18 hr were determined by flow cytometry. **(c)** Alexa-labelled ST (red) was co-injected with PBS, FL-WRS, or mini-WRS into LysM-GFP transgenic mice ears. GFP-expressing cells that co-localized with red fluorescence were captured by *in vivo* imaging system at 2 hr following ST inoculation. The number of phagocytic cells was counted in 5 different fields and the percentage of phagocytic cells were calculated (>200 cells in each group). **(d)** BMDMs were treated with 100 nM of FL- and mini-WRS for 18 hr, then incubated with FITC-labelled *E. coli* for 2 hr. Phagocytosis of the particles were measured by Vybrant phagocytosis assay kit. Data are represented as mean ± SD of triplicate measurements (a and d). *$p<0.05$, **$p<0.01$, ***$p<0.001$ compared with each control (one-way ANOVA). For panels b and c, experiments were repeated three times

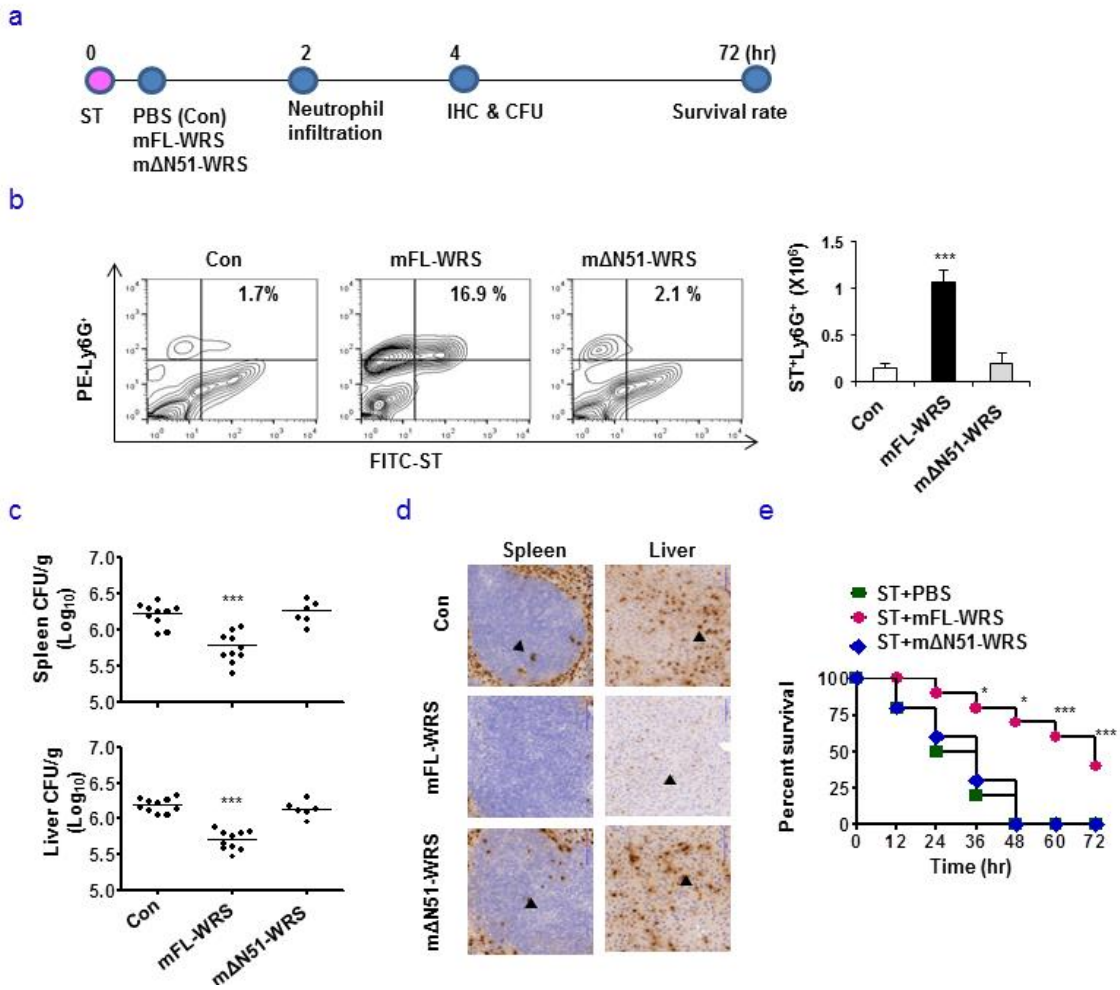

Figure II-4. FL-WRS Protects Bacteria-Infected Mice from Lethality. (a) Experimental scheme. The mice were *i.p.* injected with PBS, mFL-WRS, or mΔ51-WRS (each 20 μg/mouse) at 5 min after peritoneal *Salmonella typhimurium* (ST) inoculation ($1x10^7$ CFU). IHC; immunohistochemistry, CFU; colony

forming unit. **(b)** Mice (n=10) were inoculated with FITC-labelled ST for 2 hr, and the percentage of peritoneal $Ly6G^+$ neutrophils were analyzed by flow cytometry **(c)** Bacterial load (n=6-10) and **(d)** IHC against ST in spleen and liver of mice at 4 hr after ST inoculation. Arrows indicate ST. **(e)** Survival rates of ST-infected mice (n=10) treated with PBS, mFL-WRS (pink) and mΔN51-WRS (blue). Data are represented as mean ± SEM (b and c) or mean (e). *$p<0.05$, **$p<0.01$, ***$p<0.001$ compared with each control (one-way ANOVA).

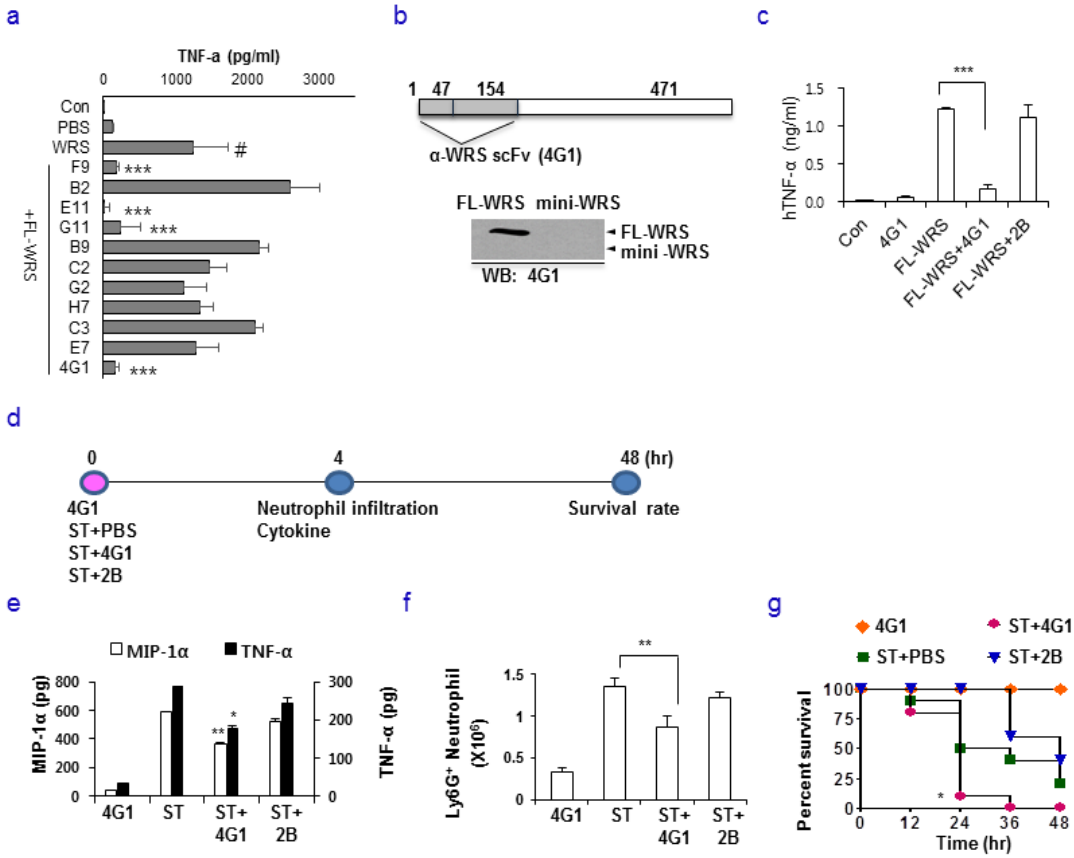

Figure II-5. Neutralization of FL-WRS aggravates bacterial infection (a) A phage-displayed scFv library was panned against surface-immobilized N154. After panning, the output clones were screened by ELISA for their binding to N154 and mini-WRS (negative control). Neutralizing activity of selected human

scFv antibodies were measured. Pre-mixed scFvs (10 μg/mL) and FL-WRS (30 nM) were treated in PMA-differentiated THP-1 cells for 3 hr. The levels of TNF-α were measured by ELISA. **(b)** Western blot analysis of recombinant human FL-WRS and mini-WRS using anti-WRS scFv 4G1. Experiments were performed in duplicate. **(c)** Neutralization of scFv 4G1 against FL-WRS reduced TNF-α production in PMA-differentiated THP-1 cells. FL-WRS (30 nM) and/or scFv 4G1 (5 μg/mL) were incubated for 2 hr at room temperature and treated for 3 hr. The levels of TNF-α were measured by ELISA. Neutralization of scFv 2B against FL-WRS did not affect TNF-α production **(d)** Experimental scheme. The mice were injected with PBS, mFL-WRS, or mΔ51-WRS (each 20 μg/mouse) and then *Salmonella typhimurium* (ST, $1x10^7$ CFU) were *i.p.* injected. **(e)** The levels of TNF-α and MIP-1α and **(h)** the number of PECs expressing $Ly6G^+$ in the

peritoneal exudates were determined by ELISA and flow cytometry, respectively. **(f)** Survival rates of ST-infected mice (n=10) treated with PBS, scFv 4G1 (pink), or scFv 2B (blue). The uninfected mice (n=10) treated with 4G1 alone were used as the negative control (orange). Data are represented as mean ± SEM (e, f, and g) or mean (a and c). *p<0.05, **p<0.01, ***p<0.001 compared with each control (one-way ANOVA).

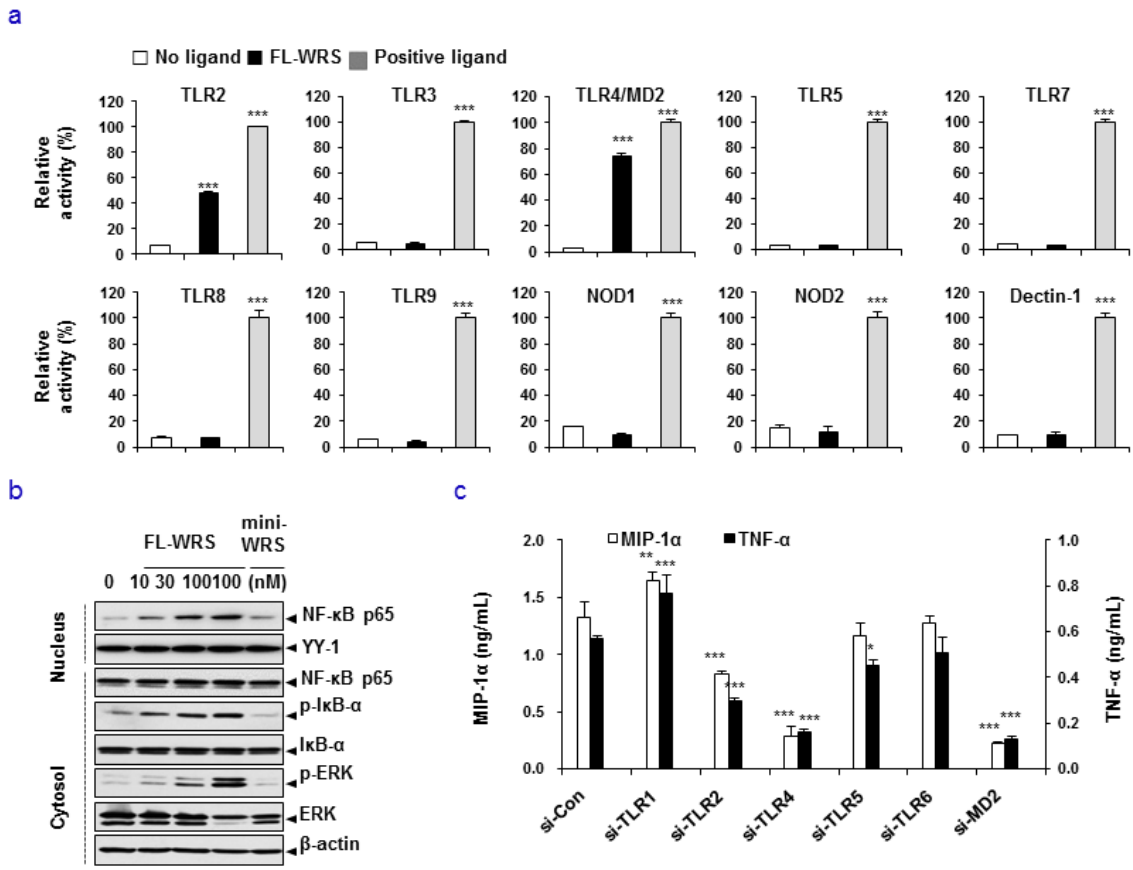

Figure III-1. Immune Activation Mechanism of FL-WRS via TLR4-MD2. (a) HEK293 cells expressing various PRRs and NF-κB SEAP reporter system were treated with FL-WRS (100 nM) for 18 hr. The relative activity of alkaline phosphatase was calculated by comparing that of cells treated with each positive control. **(b)** Western blot analysis of nuclear and cytosolic fractions from J774A.1

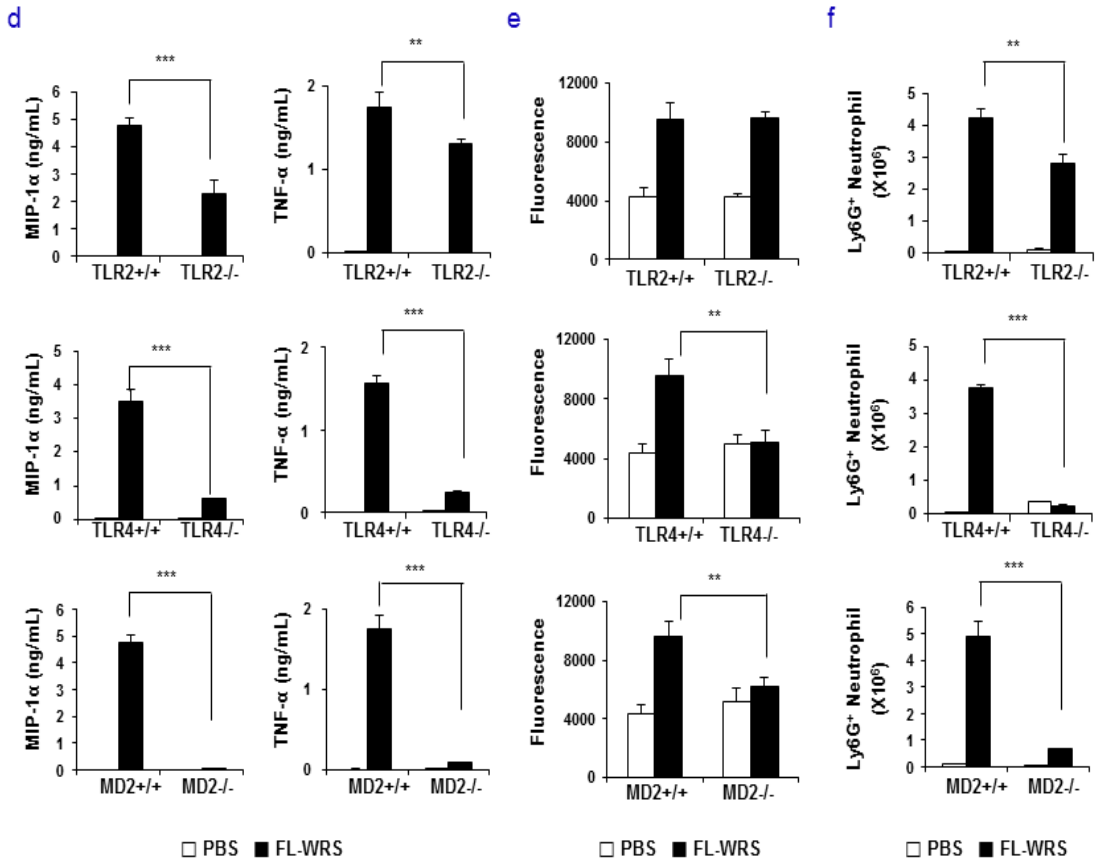

cells treated with FL-WRS and mini- WRS for 30 min. YY-1 and β-actin were used as loading controls of nucleus and cytoplasm, respectively. **(c)** TLRs were silenced in BMDMs using their respective siRNAs for 48 hr followed by FL-WRS (100 nM) treatment for 18 hr. The levels of TNF-α and MIP-1α in the culture supernatants were measured by ELISA. Scramble siRNA was used as a negative control. **(d)** BMDMs prepared from bone marrow of TLR2$^{-/-}$, TLR4$^{-/-}$, and MD2$^{-/-}$

mice were treated with FL-WRS (100 nM) and PBS for 18 hr. Levels of MIP-1α and TNF-α in the cell culture supernatant were measured by ELISA and **(e)** phagocytosis of FITC-labelled *E. coli* for 2 hr was determined by Vybrant phagocytosis assay kit. **(f)** $TLR2^{+/+}$, $TLR4^{+/+}$, and $MD2^{+/+}$ mice (n=10) were *i.p.* injected with FL-WRS (20 g/mouse) or PBS for 4 hr, and the number of $Ly6G^{+}$ neutrophils in the PECs was determined by flow cytometry. For panels a, c, and d, data are represented as mean ± SD of triplicate measurements with *p<0.05, **p<0.01, ***p<0.001 (one-way ANOVA). For panels e and f, data are represented as mean ± SEM with **p<0.01, ***p<0.001 vs those of $TLR2^{+/+}$, $TLR4^{+/+}$, and $MD2^{+/+}$ mice (one-way ANOVA). For panels b, e, and f, experiments were repeated two or three times.

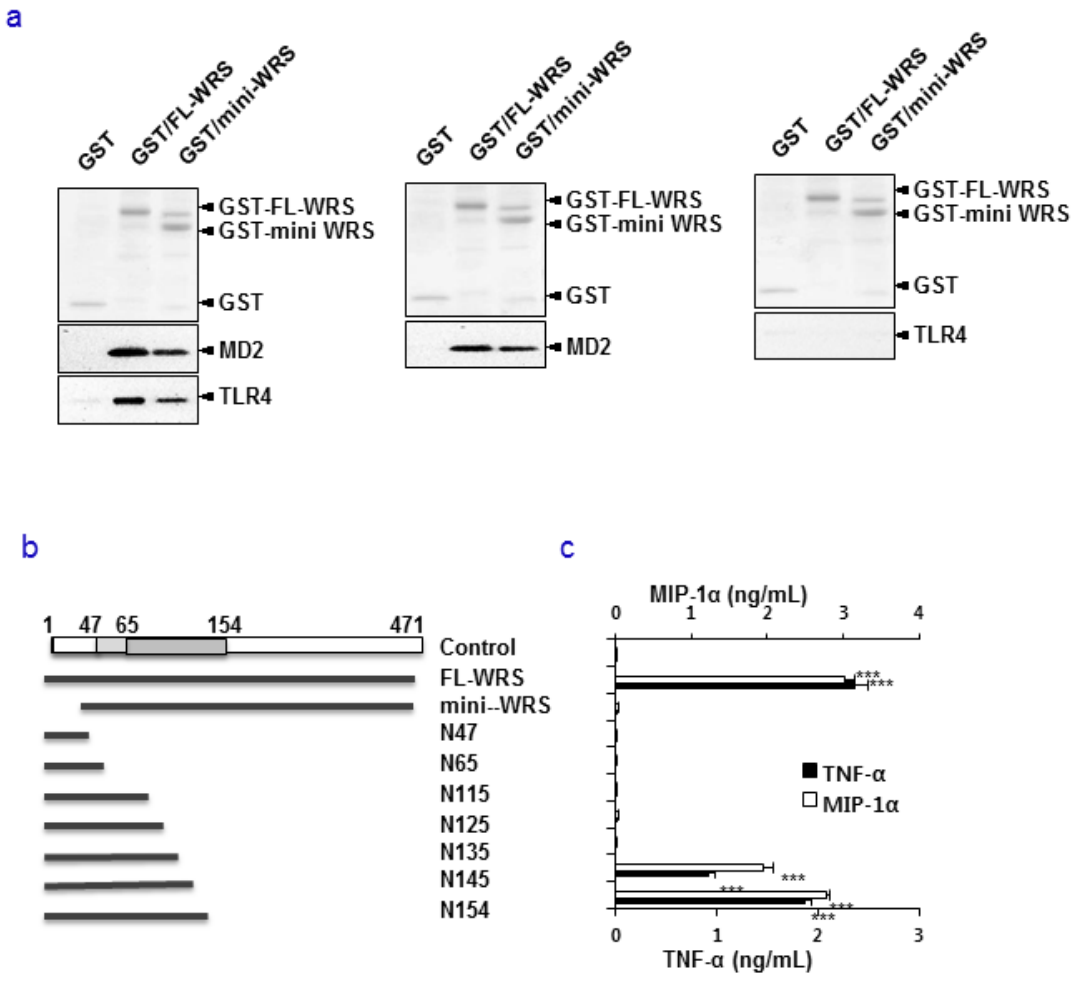
a
GST
GST/FL-WRS
GST/mini-WRS
GST-FL-WRS
GST-mini WRS
GST
MD2
TLR4
b
1
47
65
154
471
Control
FL-WRS
mini--WRS
N47
N65
N115
N125
N135
N145
N154
c
MIP-1α (ng/mL)
TNF-α
MIP-1α
TNF-α (ng/mL)

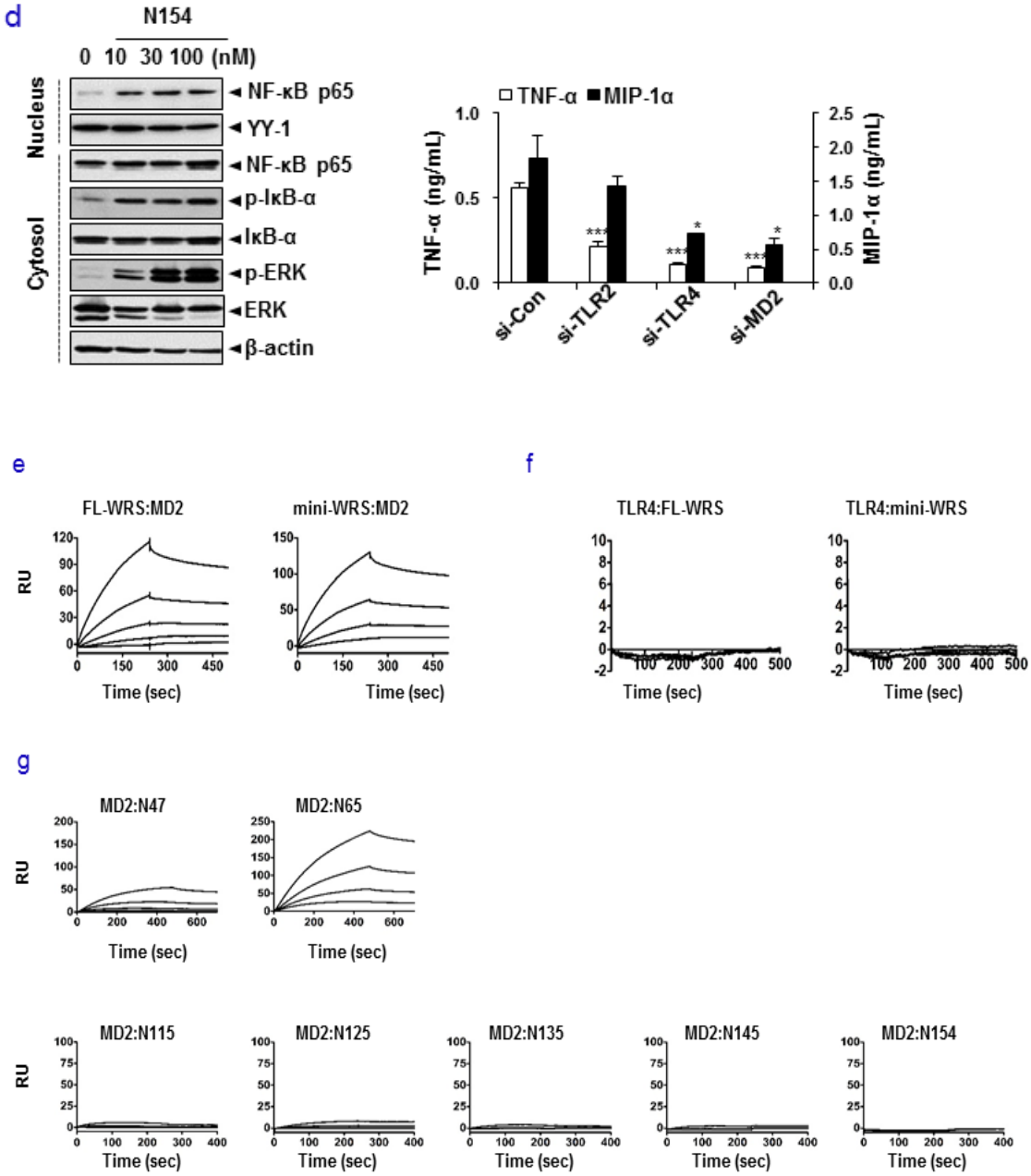
d
N154
0 10 30 100 (nM)
Nucleus
Cytosol
NF-κB p65
YY-1
NF-κB p65
p-IκB-α
IκB-α
p-ERK
ERK
β-actin
TNF-α
MIP-1α
TNF-α (ng/mL)
MIP-1α (ng/mL)
si-Con
si-TLR2
si-TLR4
si-MD2
e
FL-WRS:MD2
mini-WRS:MD2
RU
Time (sec)
f
TLR4:FL-WRS
TLR4:mini-WRS
Time (sec)
g
MD2:N47
MD2:N65
MD2:N115
MD2:N125
MD2:N135
MD2:N145
MD2:N154
RU
Time (sec)

h

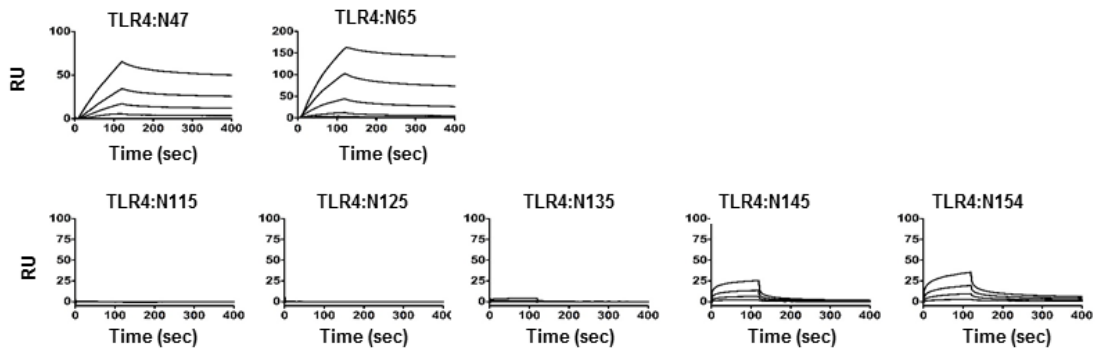

i

WRS	TLR4 Binding	MD2 Binding
-	-	-
FL (N471)	-	+
Mini (Δ47)	-	+
N47	+	+
N65	+	+
N115	-	-
N125	-	-
N135	-	-
N145	+	-
N154	+	-

Figure III-2. Binding of FL-WRS, mini-WRS and N-terminal Peptides to TLR4 and MD2 (a) GST pull-down assay**.** GST-tagged FL-WRS or mini-WRS were pre-incubated with H is-tagged MD2, and then TLR4 (2 μg each) was added. **(b)** Schematic diagram of FL-WRS, mini-WRS and series of N-terminal peptides. **(c)** The levels of

TNF-α and MIP-1α were measured by ELISA in the culture supernatants of BMDMs treated with FL-WRS, mini-WRS, and series of N-terminal peptides (100 nM each) for 18 hr. **(d)** Activation of NF-κB signaling by N154. J774A.1 cells were treated with N154 for 30 min and the levels of various proteins involved in NF-kB activation were detected by western blot analysis. In the right panel, BMDMs were transfected with each indicated siRNA for 48 hr and then treated with N154 (100 nM) for 18 hr. **(e)** FL-WRS or mini-WRS was embedded on the chip and MD2 (1.5, 0.75, 0.37, 0.19, and 0.09 μM) was flowed over as an analyte. TLR4 was embedded on the chip and **(f)** FL-WRS or mini-WRS (3, 1.5, 0.75, and 0.37 μM) was flowed over as an analyte. MD2 was embedded on the chip and **(g)** N47, N65, N115, N125, N135, N145, and N154 (3, 1.5, 0.75, and 0.37 μM) were flowed over as analytes. TLR4 was embedded on the chip and **(h)** N47, N65, N115, N125, N135, N145, and N154 (3, 1.5, 0.75, and 0.37 μM) were flowed over as analytes. **(i)** Summary of SPR analysis for binding activities of N-terminal peptides with TLR4 or MD2. For panels c and d, data are represented as mean ± SD of triplicate samples with the statistical significance of *$p<0.05$, **$p<0.01$, ***$p<0.001$ against the control and FL-WRS (one-way ANOVA), respectively.

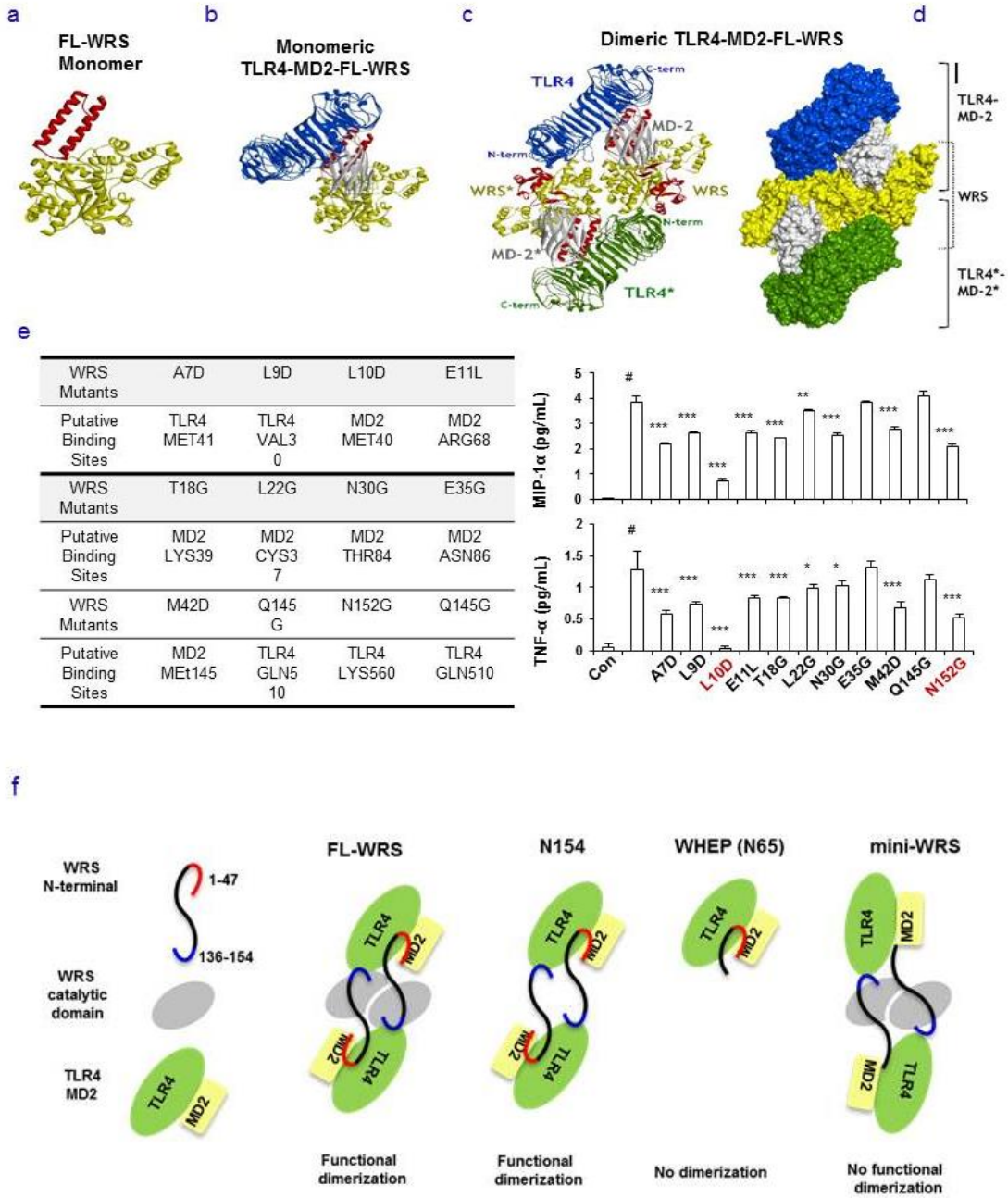

WRS Mutants	A7D	L9D	L10D	E11L
Putative Binding Sites	TLR4 MET41	TLR4 VAL330	MD2 MET40	MD2 ARG68
WRS Mutants	T18G	L22G	N30G	E35G
Putative Binding Sites	MD2 LYS39	MD2 CYS37	MD2 THR84	MD2 ASN86
WRS Mutants	M42D	Q145G	N152G	Q145G
Putative Binding Sites	MD2 MEt145	TLR4 GLN510	TLR4 LYS560	TLR4 GLN510

Figure III-3. Modeling study of FL-WRS for TLR4-MD2 Activation (a-c)

Putative binding model of TLR4-MD2 with WRS homodimer based on protein-protein docking study **(a)** The crystal structure of FL-WRS (PDB code 1R6T) monomer. The structural information of N1-6 aa and 61-81 aa peptides are missing. The helix-turn-helix WHEP domain spanning 8-64 aa is shown in red. **(b)** Potential complex formation between TLR4-MD2 (blue and grey, respectively, PDB code 3FXI) and WRS monomer (yellow). The peptide region spanning WHEP domain (red) is predicted to make interactions with both TLR4 and MD2. **(c)** Based on the model, TLR4-MD2 dimerization can be facilitated by bivalent interaction of the N154 peptides to two TLR4-MD2 units (blue and green) *in trans*. The two TLR4 interaction sites in N154 are shown (red) in ribbon type presentation. **(d)** The complex structure of the 2:2:2 TLR4-MD2-WRS is represented in surface type. **(e)** Mutations in the putative binding residues of FL-

WRS and TLR4-MD2. The levels of TNF-α and MIP-1α were measured by ELISA in the culture supernatants of BMDMs treated with WRS mutants (100 nM) for 18 hr. **(f)** Cartoon illustration explains how FL-WRS and N154 can activate TLR4-MD2 but not N65 (WHEP) and mini-WRS homodimer, based on modeling studies and functional analysis results. For panels e, data are represented as mean ± SD of triplicate samples with the statistical significance of *$p<0.05$, **$p<0.01$, ***$p<0.001$ against the control and FL-WRS (one-way ANOVA), respectively.

Table 1. Comparative distributions of sepsis-causing pathogens.

Gram(-) bacteria	N	Gram(+) bacteria	N
Acinetobacter baumanii	1	*Enterococcus faecalis*	2
Acinetobacter baumanii (CRAB)	7	*Enterococcus faecalis* (VRE)	1
Acinetobacter baumanii (CSAB)	2	*Staphylococcus aureus* (MRSA)	14
Aeromona hydrophila	3	*Staphylococcus aureus* (MSSA)	3
Burkholderia cepacia	2	*Staphylococcus epidermidis*	1
Enterobacter aerogenes	1	*Streptococcus pneumoniae*	3
Enterobacter cloacae	1	*Streptococcus agalactiae*	1
Escherichia coli	21		
Haemophilus Influenza	1		
Klebsiella pneumonia	13		
Morganella morganii	1		
Proteus mirabilis	1		
Stenotrophomonas maltophilia	1		
*Pseudomonas aeruginosa (*CRPA)	1		
Pseudomonas fluorescens	4		
Vibrio vulnificus	2		

Fungi	N	Multi-infection	N
Candida albican	2	*CRAB, E. coli*	1
Candida galabrata	1	*CRAB, P. mirabilis*	1
Bowel perfor-candida tropicalis	1	*K. pneumonia, Citrobacter*	1
Aspergillus	3	*K. pneumonia, E. coli*	1
		*K. pneumonia, A. baumanii (*CRAB)	1
		K. pneumonia, P. aeruginosa	1
		E. Coli, P. aerunginosa (CSPA)	1
		MRSA, *A. baumanii*	1
		MRSA, ESBL, *Serratia*	1
		Enterococcus, Bacteriodes, Streptococcus	1
		Fungus + MRSA	1
		unknown	3

The frequencies of Gram-negative, Gram-positive, fungi, multi-infection, and unidentified were 57.4%, 23.15%, 6.48%, 10.19%, and 2.78%, respectively

Table 2. Gene specific primer sequences for qRT-PCR and RT-PCR.

	Gene Name	Oligonucleotide Sequence
qRT-PCR	hTNF-α-F	5’-GGAGAAGGGTGACCGACTCA-3’
	hTNF-α-R	5’-CTGCCCAGACTCGGCAA-3’
	hWRS-F	5’-AAGAATTCATGCCCAACAGTGAGCCC-3’
	hWRS-R	5’-AACTCGAGCTACCCTGGAGGACAGTCAGCCTT-3’
	human β-actin-F	5′- CATGTACGTTGCTATCCAGGC-3′
	human β-actin-R	5′- CTCCTTAATGTCACGCACGAT-3′
RT-PCR	hMIP-1α-F	5’-ACCATGGCTCTCTGCAACCA-3’
	hMIP-1α-R	5’-TTAAGAAGAGTCCCACAGTG-3’
	hMIP-1β-F	5’-AGCCTCACCTCTGAGAAAACC-3’
	hMIP-1β-R	5’-GCAACAGCAGAGAAACAGTGAC-3’
	hTNF-α	primer kit (Bioneer Corp., Daejeon, Republic of Korea)
	Human β-actin-F	5′-CATGTACGTTGCTATCCAGGC-3′
	human β-actin-R	5′-CTCCTTAATGTCACGCACGAT-3′

	mMIP-1α-F	5′-TCTGCAACCAAGTCTTCTCAG-3′
	mMIP-1α-R	5′-GAAGAGTCCCTCGATGTGGGCTA-3′
	mMCP1-F	5′-CAGCAGGTGTCCCAAAGA-3′
	mMCP1-R	5′-CTTGAGGTGGTTGTGGAAA-3′
	mTNF-α-F	5′-CTCCCAGGTTCTCTTCAAGG-3′
	mTNF-α-R	5′-TGGAAGACTCCTCCCAGGTA-3′
	mouse β-actin-F	5′-ACCGTGAAAAGATGACCCAG-3′
	mouse β-actin-R	5′-TCTCAGCTGTGGTGGTGAAG-3′

Discussion

Human immune system has developed multi-layered mechanisms through evolutionary processes to win the battle against microbial infection. The first-line immune defense directly destroys invading pathogens within minutes, but if it fails, innate immune cellular responses are activated. Although exogenous ligands specific to different TLRs are well determined (Takeuchi and Akira, 2010), an infection-specific endogenous TLR activator has not yet been determined in human. This work provides several evidences suggesting human FL-WRS as a novel endogenous ligand of TLR4, promptly alerting innate immunity against infection. First, the secretion of FL-WRS would result from endocytosis of

infectious agents (Figure II-1), rather than indirectly triggered by pro-inflammatory stimuli. It is supported by the fact that WRS secretion into the blood is specifically observed in patients with sepsis but not with SIRS and chronic status of autoimmune diseases (Figure I-1). In contrast, extracellular release of HMGB-1 occurs not only by infection (Wang et al., 1999), but also by various inflammatory disorders (Harris et al., 2012) and HSP70 is induced by SIRS regardless of infection (Sonna et al., 2010) . Second, FL-WRS promptly responds to pathogens prior to onset of innate immune responses. Since FL-WRS is constitutively present in cells, it can be immediately released from monocytes, which are the first responding cells to infection, without *de novo* synthesis that is usually required for the secretion of the known cytokines for innate immunity.

Third, FL-WRS secretion can be induced by diverse pathogens (Figure I-3 and II-1), which could provide immunological flexibility. Fourth, FL-WRS appears to work primarily via TLR4 and possibly via TLR2. Through these receptors, FL-WRS could simultaneously sensitize strong and diverse immunological responses (Sato et al., 2000). Fifth, FL-WRS primarily elicits its action to macrophages. As a result, FL-WRS may not only increase phagocytosis *in situ* but also clear pathogens by enhancing neutrophil infiltration via chemokines. With these features, FL-WRS appears to suppress the propagation of infected pathogens at early stage while priming innate immune responses.

It is intriguing that both of FL-WRS and mini-WRS could bind to TLR4-MD2 while mini-WRS is completely inactive in the induction of cytokines. Perhaps, the

N-terminal 47 aa that is lacking in mini-WRS may be necessary for the right orientation of the TLR4-MD2 dimers that is required for the activation of downstream signal pathways. In fact, N47 forms a part of WHEP domain existing in the structures of several different ARSs and it is implicated in the modulation of various protein-protein interactions and immune reactions(Guo et al., 2010). The binding model and mutational analysis also explain why the peptides containing a partial or full WHEP domain of WRS (N47, N65) are not active despite the fact that they could bind to both of TLR4 and MD2. The bivalent ability of the N154 interacting two TLR4-MD2 complexes (via the WHEP domain and addition site in downstream) *in trans* appears to be necessary to work as the active ligand. It is not clear why N154 peptide was attached to the catalytic domain of WRS while it can

work as the fully functional ligand. One possibility is that N154 can secure its presence as a defense factor by being connected to WRS that is indispensable for cell viability. Another possibility is that the catalytic domain of WRS can also play an additional role in the immunological responses against infection.

Although mini-WRS was inactive in innate immunity, it was previously shown to play potent anti-angiogenic activity upon secretion. In this case, N47 needs to be cleaved off in order to expose the active site cleft of WRS to the protuberant tryptophan present in the ligand-binding domain of VE-cadherin, the functional receptor of mini-WRS (Zhou et al., 2010). However, the active role of FL-WRS and its N-terminal peptide itself has not been reported yet and here I found its active role as an endogenous activator of TLR4. Perhaps the anti-angiogenic

activity of the N-terminal truncated mini-WRS would be necessary to prevent chronic inflammation that may be caused by the sustained secretion of FL-WRS. At this point, it is not clear whether FL-WRS would work as it is or it is cleaved to generate the N154 peptide, which then activates TLR4 signal at physiological situation. N154 contains WHEP domain in its N-terminal end and this domain plays a crucial role in the binding to TLR4-MD2. Since several different ARSs also contain WHEP domains in their structures, it would be interesting to see whether other ARSs could do similar function as WRS. In this regard, it is worth noting that WRS is specifically secreted out to serum in the infected patients although GRS also contains WHEP domain, a conserved domain of helix-turn-helix domain found in WRS, HRS, EPRS, GRS and TRS.

It is not clear at this moment whether FL-WRS should be considered as a new component of innate immunity or as a distinct defensive mechanism that would prime innate immunity at the early stage of infection. Considering that FL-WRS uses TLR4 as a functional receptor, it can be recognized as an extension of innate immunity. However, FL-WRS can be considered as a unique defense factor recruited from protein synthesis machinery. It would be interesting to investigate whether the catalytic activity of WRS would be involved in its extracellular activity. In any case, this work first reports the functional connection of a protein synthesis enzyme to host defense mechanism against infection. This finding also suggests that WRS can be used as an early biomarker and also as an immune stimulant against infection.

Conclusion and Perspectives

The N-terminal truncated form of a protein synthesis enzyme, tryptophanyl-tRNA synthetase (mini-WRS) is secreted as an angiostatic ligand. However, the secretion and function of the full-length WRS (FL-WRS) remain unknown. Here we report that the FL-WRS, but not mini-WRS, is rapidly secreted upon pathogen infection to prime innate immunity. Blood levels of FL-WRS were increased in the sepsis patients, but not in those with sterile inflammation. FL-WRS was secreted from monocytes and directly bound to macrophages via toll-like receptor 4 (TLR4)-myeloid differentiation factor 2 (MD2) complex to induce phagocytosis and chemokine production. Administration of FL-WRS into *Salmonella*

Typhimurium–infected mice reduced the bacteria and improved mouse survival, whereas its titration with the specific antibody aggravated the infection. The N-terminal 154 amino acid eukaryote-specific peptide of WRS was sufficient to recapitulate FL-WRS activity and its interaction mode with TLR4-MD2 is suggested. Based on these results, secretion of FL-WRS appears to work as a primary defense system against infection, acting prior to full activation of innate immunity.

In this study, I investigate an active role of FL-WRS, not mini-WRS, as an endogenous activator of TLR4. However, it is possible that the anti-angiogenic activity of the N-terminal truncated mini-WRS serves as a feedback mechanism to prevent chronic inflammation that may be caused by the sustained secretion of FL-WRS. The early secretion of FL-WRS (starting 15 min post-infection and peaking in 1-2 hr) suggests it could serve as an early biomarker for the detection

of infections such as sepsis. Moreover, injection of FL-WRS led to pathogen clearance and improved survival in infected mice, suggesting that FL-WRS or its eukaryotic-specific N-terminal peptide could be developed as a novel therapeutic agent against diverse pathogenic challenges.

Materials and Methods

Human Samples

Serum samples were collected from 20 healthy controls, 108 septic patients receiving intensive care for sepsis, and 25 SIRS patients without infection. All patients had been admitted to the ICU of a university-affiliated hospital in Republic of Korea and only patients with proven bacterial and fungal infection were enrolled. The diagnosis of sepsis was based on the criteria presented at the

ACCP/SCCM Consensus Conference in 1992(Bone et al., 1992). This study was approved by the Institutional Review Board of the Asan Medical Hospital (2011-0001).

Total 52 subjects, who were admitted to the Severance Hospital Allergy-Asthma Clinics from January 2014 to July 2015, were enrolled. The enrolled subjects included 22 healthy control and 30 stable asthma patients who were diagnosed as asthma by allergy specialists, based on their symptoms and pulmonary function test results (>12% increase of forced expiratory volume for 1 second (FEV1) after bronchodilator use. This clinical study was approved by the Institutional Review Board, Severance Hospital and Yonsei University Health System (approval number: 4-2013-0397).

Sera were obtained from 45 patients with primary Sjogren's syndrome, 30

patients with rheumatoid arthritis (RA) and 15 healthy controls. Primary Sjogren's syndrome was diagnosed according to the American-European Consensus Group criteria for primary Sjogren's syndrome(Vitali et al., 2002) or the 2012 American College of Rheumatology criteria(Shiboski et al., 2012). RA was diagnosed according to 1987 revised criteria for the classification of rheumatoid arthritis(Arnett et al., 1988) or 2010 rheumatoid arthritis classification criteria(Aletaha et al., 2010). This study was approved by the Institutional Review Board of Seoul St. Mary's Hospital (KC13ONMI0646). All human serums were obtained under informed consent.

Reagents and Assay Kits

Anti-TNF-α (Cat. No 3707), anti-HMGB1 (Cat. No 3935), anti-HSP70 (Cat. No

4872), anti-NF-κBp65 (Cat. No 3034), anti-p-IκB-α (Cat. No 9246), anti-p-ERK (Cat. No 9101), anti-ERK (Cat. No 9102), and anti-His-tag (Cat. No 12689) were purchased from Cell Signaling Technology. Anti-CD11b-FITC (M1/70, Cat. No 553310), anti-LY6G and Ly6C-PE (RB6-8C5, Cat. No 553128), CD40-PE (3/23, Cat. No 553791), CD80-PE (16-10A1, Cat. No 553769), and CD86-FITC (GL1, Cat. No 553691) were from BD Pharmingen. Anti-F4/80-PE (BM8, eBioscience, Cat. No 12-4801-80), TLR4 (R&D systems, Cat. No 1478-TR) and MD2 recombinant proteins (R&D systems, Cat. No 1787-MD) were also purchased. Anti-WRS (Cat. No NMS-01-0009,), anti-MRS (NMS-01-0003), anti-HRS(Park et al., 2005), anti-GRS (NMS-01-0014), anti-KRS (NMS-02-0005), anti-DRS (NMS-01-0013) and anti-AIMP1 (NMS-01-0019) antibody were purchased from Neomics (Suwon, Republic of Korea). BrdU cell proliferation assay kit (Cell

Signaling Technology, Cat. No 6813), Lactate dehydrogenase (LDH) cytotoxicity detection kit (Takara, Cat No MK401), Vybrant phagocytosis assay kit (Cat. No V6694), ELISA kits for human WRS (Cusabio, Cat. No CSB-E11789h), GRS (Cusabio, Cat. No CSB-EL009262hu), KRS (MyBiosource, Cat. No MBS067424), murine WRS (Cloud Clone Corp, Cat. No SEB748mu), human HMGB-1 (Cloud Clone Corp, Cat. No SEA399hu), human HSP70 (Cloud Clone Corp, Cat. No SED506hu), human MIP-1α (R&D systems, Cat. No DY270), human MIP-1β (R&D systems, Cat. No DY271), human TNF-α (eBioscience, Cat. No 88-7346-88), murine MIP-1α (R&D systems, Cat. No DY150), murine MCP-1 (R&D systems, Cat. No DY479), and murine TNF-α (eBioscience, Cat. No 88-7324-88) were purchased. Each assay was performed according to manufacturer's protocol. Human TLR1-9 Agonist Kit (Invivogen, Cat. No tlr1-kit1hw), zymosan (Sigma,

Cat. No Z4250), human TNF-α Peprotech, Cat. No 300-01A), nigericin (Sigma, Cat. No N7143), cytochalacin D (Sigma, Cat. No C2618), dynasore (Sigma, Cat. No D7693), and polystyrene latex beads (Sigma, LB30) were purchased. Dr. Honggu Chun (Korea University, Republic of Korea) kindly provided liposome (200 nm size).

Bacteria, Fungus, and Virus

Salmonella typhimurium (ATCC 14028), *Listeria monocytogenes* (ATCC 15313), *Escherichia coli*-K12 (ATCC 10798), *Staphylococcus aureus* (ATCC 25923), and *Candida albicans* (ATCC 10231) were obtained from Korean Culture Center of Microorganisms (Seoul, Republic of Korea). The number of overnight cultured bacteria and fungus were estimated from the absorbance at 600 nm using a

predetermined calibration curve. Respiratory syncytia virus(RSV) A2 virus was propagated by inoculating with human larynx carcinoma cell line, HEp-2 (CCL-23), monolayer with a previously prepared small-scale isolate stock (MOI=0.01) and harvested when cytopathic effects were greater than 60%. Influenza A/Puerto Rico/8/1934 virus was propagated in specific pathogen-free embryonated eggs. Viruses were titrated by standard plaque assay.

Cell Culture

Human PBMCs were isolated by Cell Preparation Tube with sodium citrate (Becton Dickinson, Cat. No 362761). The human bloods were obtained from healthy volunteers and the protocol was approved by the Institutional Review Board at Seoul National University (approval number: 1502/001-010). Human B

(Cat. No 130-101-638), T (Cat. No 130-096-olp; 535), NK (Cat. No 130-092-657), and monocyte (Cat. No 130-091-153) were prepared from human PBMC using magnetic activated cell sorting (MACS, Miltenyi Biotec). Mouse B (Cat. No 130-090-862) and T cells (Cat. No 130-090-860) were prepared from mouse spleen. Mouse NK cells (Cat. No 130-096-892), monocyte (Cat. No 130-100-629) and neutrophil (Cat. No 130-097-658) were prepared from MACS. BMDMs were differentiated from mouse bone marrow cells for 6-7 days with M-CSF (Peprotech, Cat. No 315-02, 20 ng/mL). All isolated and cultured cells were determined by cell surface marker expression using FACS analysis.

The HEK293T (human embryonic kidney 293T cell line, ATCC® CRL-3216™), THP-1 (human monocytic cell line, ATCC® TIB-202™) and J774A.1 (murine macrophage cell line, ATCC® TIB-67™) were purchased from American Type

Culture Collection (Manassas, VA, USA). The HEK293T and J774A.1 cells were grown in Dulbecco's Modified Eagle's Medium (DMEM) containing 10% fetal bovine serum (FBS) and 1% streptomycin and penicillin. THP-1 cell lines were grown in RPMI-1640 medium containing 10% fetal bovine serum (FBS), 1% streptomycin and penicillin, and 50 μM β-mercaptoethanol. Mycoplasma contamination was tested by commercially available mycoplasma detection kit (Takara, Cat. No 6601).

ELISA

The levels of WRS, GRS, KRS, HMGB1, HSP70, TNF-α, MIP-1α, MIP-1β, and MCP-1in the cell culture supernatants, peritoneal exudates lavage, and human serums were determined using commercially available ELISA kits according to

manufacturer's protocol.

WRS protein precipitation by TCA

Human PBMCs (2X10^6/mL) were seeded in 60pi dish in RPMI media containing 1~2% FBS for 2hrs. *S. typhimurium*, suspended in serum free media, was added in the cultured hPBMCs. The culture media was collected and centrifuged at 500Xg, 4℃ for 10min. And then collected the supernant was re-centrifuged at 10,000Xg, 4℃ for 10min. 100μL of 100% TCA solution was added into 900μL supernant to make 10% of total volume and incubated the tube in 4 ℃ over-night. After one day from 4 ℃ incubation, centrifuge the tube at 20,000Xg for 30min. Remove all media with vacuum suction. Add 200~240 ㎕

pH8.0 100mM HEPES and 50-60 $\mu\ell$ 5Xsds sample loading dye into the tube. Boil the sample for 15min and load the gel for Western blot.

Western Blot Analysis

Cytosolic and nuclear extracts were prepared using a Nuclear Extract kit (Active Motif, Cat. No 40010), and Western blot analysis was performed according to the methods previously described (Park et al., 2014) using specific antibodies.

Recombinant Protein Purification

A series of human WRSs, N-terminal peptides, mutant WRSs, murine FL-WRS (mFL-WRS), and the N-terminal 51aa-deleted WRS (mΔN51-WRS) were cloned in pET-28a (His-tag) vector. WRS mutants were generated by site-directed

mutagenesis kit (Agilent Technologies). The recombinant proteins were overexpressed in *E. coli* Rosetta2 (DE3) strain. The bacterial cells were lysed by sonication 3 times (10 sec duration with 50 sec interval). His-tagged proteins in supernatants were purified using HiTrap HP column (GE Healthcare), followed by HiLoad 16/600 Superdex 200 prep grade column (GE Healthcare Life Sciences). GST-tagged proteins were purified by Glutathione-Sepharose high performance beads (GE Healthcare Life Sciences). Purified proteins were filtered using Mustang E membrane (Pall Corporation). For preparation of the recombinant proteins from HEK293T cells, human *FL-WRS* and *mini-WRS* were cloned into pEXPR-IBA42 vector (IBA, Cat. No 2-1942-000) designed for the expression in cell culture supernatant. FL-WRS and mini-WRS were expressed in HEK293T cells for 48 hr and purified from the cell culture supernatants using Ni-NTA resin

(Invitrogen).

RT-PCR and Real Time-PCR

RNAs were extracted according to the protocol of the RNeasy kit (Qiagen, Cat. No 74104), and the RNA samples were used for cDNA synthesis using a PrimeScript RT reagent kit (TaKaRa, Cat. No PR037A). Quantitative RT-PCR was quantified using 7500 real-time PCR system (Applied Biosystems) with Power SYBR® Green PCR Master Mix (Applied Biosystems, Cat. No 4367659). The mRNA level of GAPDH and β-actin were used as internal control. RT-PCR was performed according to the methods previously described(Park et al., 2014). The gene specific primer sequences were shown in Table 2.

Cell Migration Assay

The cell migration assay was performed using polycarbonate membrane transwell (Costar, Cat. No 3421, 5.0 μm,) coated with gelatin. Mouse primary cells were allowed to migrate for 4 hr into lower chamber and infiltrated cells were counted under the bright field microscope.

Animal Experiments

Animal experiments complied with the guidelines of the Daejeon University Animal Care and Use Committee (approval number DJUARB2014-031). C57BL/6 mice (female, 9-10 weeks old) were purchased from Daehan Biolink Co. Ltd. (Chungbuk, Republic of Korea). Female LysM-GFP mice (Lysozyme M-GFP, kindly provided by Dr. Kim at Rochester University) were used at the ages

between 12 and 17 weeks for *in vivo* imaging experiments. $MD2^{-/-}$ mice(Nagai et al., 2002) were purchased from RIKEN BioResource Center (Ibaraki, Japan). Dr. Chul-Ho Lee and Jong Soo Lee provided the $TLR2^{-/-}$ and $TLR4^{-/-}$ mice(Hoshino et al., 1999; Takeuchi et al., 2000). Sample size (the number of mice per group) was chosen to warrant statistical significance (generally >5 mice per group) and mice were randomly distributed into their respective groups. All experiments were conducted without blinding with age and sex-matched mice. The counting of phagocytic cells in pictures obtained from *in vivo* imaging experiments were performed in a blind manner. We included all of the tested mice for analysis. The samples from each mouse were prepared as duplicate or triplicate for measurements, and the experiments were repeated two or three times.

In Vivo Bacterial Infection and Bacteria Counting

Salmonella typhimurium (ST) was grown to OD_{600}=0.5 in NB broth, washed in PBS at 10,000 x*g* and resuspended in PBS. ST was intraperitoneally infected with $1x10^7$ CFU per mouse. After 4 hr infection, spleen and liver were homogenized in 4 mL of D.W. The homogenized lysates were serially diluted to 1:10 with D.W. 10 μL of chosen dilutions were spotted four times on NB agar plates and incubated at 37℃.

FITC labeling of Bacteria

Bacterial cells were harvested by centrifugation at 10,000x g and 4℃ for 5 min and washed with PBS for two times. Measure the optical density at 600 nm of cell suspension and prepare 10^9 cells in pellet. Fluorescein isothiocyanate (FITC;

Invitrogen F-1906) was freshly dissolved with DMSO to make 10mg/mL stock solution. Dilute the FITC stock solution of 10 mg/ml to a final concentration of 0.2 mg/ml in PBS. Add 1 ml of FITC (0.2 mg/ml) solution to the microcentrifuge tube, thoroughly resuspend the bacterial pellet, and incubate for 30 min at 4◦C in the dark. Resuspend the bacteria to the desired concentration in sterile PBS and use for the infection.

Lavaging the peritoneal exudate cells (PECs)

The peritoneal cavity is lavaged 0 to 4 h after injection of WRS protein. Mice were sacrificed using carbon dioxide. Make a small (0.5 cm) incision along the midline of the abdomen allowing the skin to be pulled back to expose the abdomen. Inject 3~5 ml ice-cold PBS/5 mM EDTA washing solution with a

syringe and 5/8-inch 25-G needle. Gently massage the mouse abdomen with the length of a 2-inch 19-G needle to ensure that cells that are loosely adherent to the peritoneal wall or other organs will detach and become suspended in the lavage fluid. Use a 19-G needle to gently and slowly extract the lavage fluid from the peritoneal cavity. Transfer the fluid to a 15-ml centrifuge tube and keep on ice.

Preparation of WRS and GRS scFv

Phage-displayed human scFv library was panned against different recombinant human WRS as described previously(Yang et al., 2009). Briefly, an immunotube was coated with 10 μg of WRS and blocked with mPBS (PBS with 3% nonfat dried milk). Phage-displayed scFv library (1x 10^{13} CFU) in 1 mL of mPBST (PBST with 3% nonfat dried milk) was added to the immunotube. After 2 hr incubation, the tube was washed 3-5 times with PBST, and the bound phages were

eluted with 1 mL of 100 mM trimethylamine and neutralized with 0.5 mL of 1 M Tris-HCl (pH 7.0). ER2537 *E.coli* in mid-log phase were infected with the eluted phage, and plated on LB-ampicillin plates supplemented with 2% glucose. Next day, the bacteria were collected from the plates by adding 5 mL of LB medium to the plate and scraping the bacteria with glass spreader. Fifty microliters of the harvested bacteria were added to 20 mL SB (3% Tryptone, 2% yeast extract, 1% MOPS, pH 7.0) plus ampicillin medium and grown for 2-3 hr until OD_{600} reaches 0.5. VCSM13 helper phage ($1x10^{11}$ PFU) was added, and the infection continued for 1 hr at 37^{o}C with slow shaking. Kanamycin (70 μg/mL) was subsequently added, and the culture was incubated overnight at 30^{o}C with vigorous shaking. Next day, the culture was centrifuged, and phage precipitation solution (4% PEG8000 and 3% NaCl, final concentration) was added and mixed thoroughly.

After incubation on ice for 30 min, the precipitated phages were obtained by centrifugation and suspended in PBS, and used for the subsequent round of panning. After four rounds of panning the library, individual scFv clones were screened by ELISA for their ability to bind WRS. The positive clones were sequenced to identify unique clones, and each clone was expressed in *E.coli*, and purified by Ni-NTA affinity column. Anti-GRS scFv clone 2B had been isolated form the same synthetic scFv library as scFv 4G1 using recombinant human GRS as an antigen. The clone specifically bound to GRS in immunoblot assays.

In Vivo **Imaging System and Image Processing**

The Alexa647-labelled FL-WRS, mini-WRS (red fluorescence, each 0.1 μg) or PBS (Zhu et al.) were injected intradermally into the ear of LysM-GFP transgenic

mice. The infiltration of green fluorescence-labelled cells was monitored using *in vivo* imaging system. Time lapse imaging was performed with 30 sec intervals at 1 or 4 hr after injection (20 x magnifications). For analysis of increased phagocytosis by FL-WRS, Alexa647-labelled *Salmonella typhimurium* (ST) (red) was co-injected with PBS, FL-WRS, or mini-WRS into LysM-GFP transgenic mice ears. GFP-expressing cells that co-localized with red fluorescence were captured by *in vivo* imaging system at 2 hr following ST inoculation. The number of phagocytic cells was counted in 5 different fields and the percentage of phagocytic cells was calculated (>200 cells in each group). A custom-built video-rate laser-scanning confocal microscope imaging system modified from a previously designed system(Choe et al., 2013; Faust et al., 2000; Seo et al., 2015) was used to visualize immuno-cellular dynamics. Three continuous laser whose

wavelength was at 488 nm (MLD, Cobolt), 561 nm (Jive, Cobolt) and 640 nm (MLD, Cobolt) was used as fluorescent excitation source to achieve three-color fluorescent image. Fast-rotating 36 facet polygonal mirror (MC-5, aluminum coated, Lincoln Laser) and galvanometer mirror (Cambridge Technology, 6230H) were utilized to obtain 2D scanning pattern. Emitted three color fluorescent signals from intravital mouse model on 3D motorized XYZ translational stage (Sutter Instrument, MPC-200-ROE) were detected by high-sensitive photomultiplier tubes (Hamamatsu, R9110) and digitalized by 8-bit 3-channel frame grabber (Matrox, Solios). 20x (Olympus, LUMFLN60XW, NA1.1), and 60x objective lens (Olympus, LUCPLFLN20X, NA0.45) objective lens generated 500x500, and 167x167 μm images of field views, respectively. Images were obtained by Matrox Imaging Library (Matrox, MIL9) custom-written imaging

software with 512x512 pixels per frame at 30 Hz of frame rate, and processed by Matlab (Mathworks) for XY-shift compensation and by ImageJ software (National Institutes of Health) for XZ/YZ axis-reconstruction.

Flow Cytometry

The cells were stained with antibodies for 30 min on ice in a binding buffer (PBS with 0.5% BSA and 0.01% NaN_3) and analyzed by one- or two-color flow cytometry on FACSCalibur (BD Biosciences) using FlowJo software (Flowjo LLC).

Immunohistochemistry

Paraffin embedded sections were incubated in a solution of 0.3% H_2O_2 for 15 min to inhibit endogenous peroxidase activity. Sections were then incubated for 1 hr at

RT with primary antibodies (1:2000 diluted) against *Salmonella* antibody (Novus Biologicals, Cat. No NB600-1087). The detection systems EnVision+ for rabbit antibodies (DAKO, Glostrup, Denmark, Cat. No K4003,) were applied according to the manufacturers' instructions. Slides were stained with liquid diaminobenzidine tetrahydrochloride (DAB+), a high-sensitivity substrate-chromogen system (K3468, DAKO, Glostrup, Denmark). Counterstaining was performed with Meyer's haematoxylin. The images on the slides were visualized with an Olympus Bx40 light microscope.

Macrophage Depletion

To deplete macrophages in spleen, mice were injected *i.v.* with liposomal clodronate (1 mg/mouse, Encapsula NanoSciences LLC) for 24 hr. To deplete

macrophages in PECs, mice were simultaneously injected both *i.v.* (0.5 mg/mouse) and *i.p.* (0.75 mg/mouse) with liposomal clodronate for 24 hr. Control liposome was injected as a negative control of macrophage depletion.

PRRs Reporter Assay

HEK293 cells expressing the SEAP reporter system (Invivogen) were treated with FL-WRS or each specific ligand (positive control) for mouse PRRs for 18 hr (InvivoGen Study # 157908). The ligands are HKLM (heat-killed *L. monocytogenes*, $1x10^8$ cells/mL), poly(I:C) (1 μg/mL), *E. coli*-K12 LPS (100 ng/mL), *S. typhimurium* flagellin (ST-FLA, 100 ng/mL), CL097 (1 μg/mL), CL075 (10 μg/mL) + poly(dT) (10 μM), CpG ODN 1826 (100 ng/mL), C12-iEDAP (100 ng/mL), L18-MDP (100 ng/mL) and zymosan (hot alkali-treated *S.*

cerevisiae, 10 μg/mL).

Si-RNA Transfection

Mouse si-TLR1 (Cat. No Tlr1-MSS211916), si-TLR2 (Cat. No Tlr2-MSS216272), si-TLR4 (Cat. No Tlr-MSS211922), si-TLR5 (Cat. No Tlr5-MSS285031), si-TLR6 (Cat. No Tlr6-MSS211925) and si-MD2 (Cat. No Ly96-MSS275499) were purchased from Invitrogen. BMDMs ($1x10^5$) were plated in 48-well for overnight and transfected with si-RNAs using X-tremeGENE siRNA Transfection Reagent (Roche Diagnostics, Cat. No 04 476 093 001). Stealth universal RNAi (Invitrogen) was used as a negative control.

***In Vitro* Pull-down Assay**

FL-WRS and mini-WRS were cloned into pGEX4T-1 (GST-tag) vector. The recombinant proteins were overexpressed in *E. coli* Rosetta2 (DE3) strain. The bacterial cells were lysed by sonication 3 times (10 sec duration with 50 sec interval). GST-tagged WRSs were purified by Glutathione-Sepharose high performance beads (GE Healthcare Life Sciences). Purified proteins were filtered using Mustang E membrane (Pall Corporation). GST, GST-FL-WRS, or GST-mini-WRS (each 2 μg) in PBS were mixed with Glutathione-Sepharose beads at 4°C for 2 hr. Recombinant human TLR4 and/or MD2 (each 2 μg) proteins were added and the mixtures were incubated at 4℃ for 4 hr. Proteins binding to beads were subjected to Western blot analysis.

Surface Plasmon Resonance

Surface Plasmon Resonance (SPR) experiments were performed using a Biacore T200 (GE Healthcare) equipped with a Series S sensor chip CM5 (GE Healthcare) at 25℃. PBS buffer (KH_2PO_4 144 mg/L, NaCl 9,000 mg/L, Na_2HPO_4 795 mg/L, without calcium or magnesium) was used as a running buffer for the immobilization procedure. Immobilization was performed by using amine coupling kit (GE Healthcare). Flow cells were activated with a 7 min pulse of a 1:1 mixture of EDC (1-ethyl-3-(3-dimethylaminopropyl)carbodiimide hydrochloride) and NHS (N-Hydroxysuccinimide) according to manufacturer's recommendations. FL-WRS and mini-WRS were diluted with 10 mM sodium acetate (pH 5.0 for FL-WRS and pH 5.5 for mini-WRS) and immobilized to a Series S sensor chip CM5 to achieve immobilization levels of 600-1600 and 600-1500 RU, respectively. In another set of experiment, human TLR4 and MD2

proteins were diluted with 10 mM sodium acetate (pH 5.0) and immobilized to the chip giving a surface density of 1000-2600 and 600-1000 response units (Shen et al.), respectively. Flow cells were then blocked with a 7 min pulse of 1 M ethanolamine-HCl (pH 8.5). Serially diluted analytes or buffer were injected for 1-10 min at 30 µL/min flow rate and washed out for 20 min according to the analytes. Sensorgrams obtained with the reference channel were subtracted from those obtained with the channel with each protein.

Protein-protein Docking Study

Interaction of WRS and TLR4-MD2 of human form was simulated by using ZDOCK and RDOCK in the Discovery Studio 4.5 software package. The X-ray crystal structure of the human WRS (PDB code 1R6T) was obtained from the

Protein Data Bank. Also, TLR4-MD2 complex X-ray structure was (PDB code 3FXI) from the PDB site. To assignment CHARMM force field for protein-protein docking study, I modified selenomethionine (Mse) residue of WRS to methionine (Met) using Build Mutant protocol in Discovery Studio 4.5. I generated WRS dimer structure including N7-60 residues that chain A was superimposed on chain B. The two WRS monomers were built a symmetric structure. First step, the top 2,000 out of 54,000 docked poses of WRS dimer bound to 1:1 TLR4-MD2 were clustered and evaluated by ZDOCK. Thirteen docking models with high ZDOCK score were chosen by eye-selection for further refinement of energy optimization, a set of docked protein poses in RDOCK using CHARMM polar H force field. Three WRS dimer models bound to 1:1 TLR4-MD2 were selected. Second step, I performed docking study again with WRS

dimer bound to 1:1 TLR4-MD2 poses from previous docking study for predicting dimerization of 2:2 TLR4-MD2 linking by WRS dimer. The top 85, 82 and 93 of 54,000 respectively docked poses of 1:1 TLR4-MD2 bound to 1:1 TLR4-MD2-WRS dimer were clustered and evaluated by ZDOCK. Three high-scoring and eye-selection docking models were selected by ZDOCK analysis. For further refinement of energy optimization each set of docked protein posed by RDOCK in the same manner. I selected final possible protein-protein docking model of 2:2 TLR4-MD2 dimerization bound to WRS dimer using RDOCK energy and visual inspection

Statistics

Data are shown as means ± standard deviations (SD) or means ± standard error (SEM). Statistical significance was calculated by one-way analysis of variance

(ANOVA) following Tukey's test using SPSS software (version 21, IBM-SPSS Inc., Chicago, IL). Two-tailed Mann-Whitney test was performed using GraphPad Prism version 5.01 (GraphPad Software). $p<0.05$ was considered to be statistically significant.

References

Aletaha, D., Neogi, T., Silman, A.J., Funovits, J., Felson, D.T., Bingham, C.O., 3rd, Birnbaum, N.S., Burmester, G.R., Bykerk, V.P., Cohen, M.D., *et al.* (2010). 2010 rheumatoid arthritis classification criteria: an American College of Rheumatology/European League Against Rheumatism collaborative initiative. Annals of the rheumatic diseases *69*, 1580-1588.

Arnett, F.C., Edworthy, S.M., Bloch, D.A., McShane, D.J., Fries, J.F., Cooper, N.S., Healey, L.A., Kaplan, S.R., Liang, M.H., Luthra, H.S., and et al. (1988). The American Rheumatism Association 1987 revised criteria for the classification of rheumatoid arthritis. Arthritis and rheumatism *31*, 315-324.

Bao, Y.S., Ji, Y., Zhao, S.L., Ma, L.L., Xie, R.J., and Na, S.P. (2013). Serum levels and activity of indoleamine2,3-dioxygenase and tryptophanyl-tRNA synthetase and their association with disease severity in patients with chronic kidney disease. Biomarkers : biochemical indicators of exposure, response, and susceptibility to chemicals *18*, 379-385.

Bone, R.C., Balk, R.A., Cerra, F.B., Dellinger, R.P., Fein, A.M., Knaus, W.A., Schein, R.M., and Sibbald, W.J. (1992). Definitions for sepsis and organ failure and guidelines for the use of innovative therapies in sepsis. The ACCP/SCCM Consensus Conference Committee. American College of Chest Physicians/Society of Critical Care Medicine. Chest *101*, 1644-1655.

Brown, K.A., and Treacher, D.F. (2006). Neutrophils as potential therapeutic targets in sepsis. Discovery medicine *6*, 118-122.

Chaplin, D.D. (2010). Overview of the immune response. The Journal of allergy and clinical immunology *125*, S3-23.

Choe, K., Hwang, Y., Seo, H., and Kim, P. (2013). In vivo high spatiotemporal resolution visualization of circulating T lymphocytes in high endothelial venules of lymph nodes. Journal of biomedical optics *18*, 036005.

Dziarski, R., and Gupta, D. (2000). Role of MD-2 in TLR2- and TLR4-mediated recognition of Gram-negative and Gram-positive bacteria and activation of

chemokine genes. Journal of endotoxin research *6*, 401-405.
Ellis, C.N., LaRocque, R.C., Uddin, T., Krastins, B., Mayo-Smith, L.M., Sarracino, D., Karlsson, E.K., Rahman, A., Shirin, T., Bhuiyan, T.R., *et al.* (2015). Comparative proteomic analysis reveals activation of mucosal innate immune signaling pathways during cholera. Infection and immunity *83*, 1089-1103.
Faust, N., Varas, F., Kelly, L.M., Heck, S., and Graf, T. (2000). Insertion of enhanced green fluorescent protein into the lysozyme gene creates mice with green fluorescent granulocytes and macrophages. Blood *96*, 719-726.
Fitzgerald, K.A., Palsson-McDermott, E.M., Bowie, A.G., Jefferies, C.A., Mansell, A.S., Brady, G., Brint, E., Dunne, A., Gray, P., Harte, M.T., *et al.* (2001). Mal (MyD88-adapter-like) is required for Toll-like receptor-4 signal transduction. Nature *413*, 78-83.
Frolova, L., Sudomoina, M.A., Grigorieva, A., Zinovieva, O.L., and Kisselev, L.L. (1991). Cloning and nucleotide sequence of the structural gene encoding for human tryptophanyl-tRNA synthetase. Gene *109*, 291-296.
Ge, Q., Trieu, E.P., and Targoff, I.N. (1994). Primary structure and functional expression of human Glycyl-tRNA synthetase, an autoantigen in myositis. The Journal of biological chemistry *269*, 28790-28797.
Guo, M., Yang, X.L., and Schimmel, P. (2010). New functions of aminoacyl-tRNA synthetases beyond translation. Nature reviews. Molecular cell biology *11*, 668-674.
Harris, H.E., Andersson, U., and Pisetsky, D.S. (2012). HMGB1: a multifunctional alarmin driving autoimmune and inflammatory disease. Nature reviews. Rheumatology *8*, 195-202.
Hirakata, M., Suwa, A., Takeda, Y., Matsuoka, Y., Irimajiri, S., Targoff, I.N., Hardin, J.A., and Craft, J. (1996). Autoantibodies to glycyl-transfer RNA synthetase in myositis. Association with dermatomyositis and immunologic heterogeneity. Arthritis and rheumatism *39*, 146-151.
Hoshino, K., Takeuchi, O., Kawai, T., Sanjo, H., Ogawa, T., Takeda, Y., Takeda, K., and Akira, S. (1999). Cutting edge: Toll-like receptor 4 (TLR4)-deficient mice are hyporesponsive to lipopolysaccharide: evidence for TLR4 as the Lps gene

product. Journal of immunology *162*, 3749-3752.
Kelso, A. (1998). Cytokines: principles and prospects. Immunology and cell biology *76*, 300-317.
Kisselev, L., Frolova, L., and Haenni, A.L. (1993). Interferon inducibility of mammalian tryptophanyl-tRNA synthetase: new perspectives. Trends in biochemical sciences *18*, 263-267.
Murray, P.J., and Wynn, T.A. (2011). Protective and pathogenic functions of macrophage subsets. Nature reviews. Immunology *11*, 723-737.
Nagai, Y., Akashi, S., Nagafuku, M., Ogata, M., Iwakura, Y., Akira, S., Kitamura, T., Kosugi, A., Kimoto, M., and Miyake, K. (2002). Essential role of MD-2 in LPS responsiveness and TLR4 distribution. Nature immunology *3*, 667-672.
Park, B.S., Song, D.H., Kim, H.M., Choi, B.S., Lee, H., and Lee, J.O. (2009). The structural basis of lipopolysaccharide recognition by the TLR4-MD-2 complex. Nature *458*, 1191-1195.
Park, S., Choi, J.J., Park, B.K., Yoon, S.J., Choi, J.E., and Jin, M. (2014). Pheophytin a and chlorophyll a suppress neuroinflammatory responses in lipopolysaccharide and interferon-gamma-stimulated BV2 microglia. Life sciences *103*, 59-67.
Park, S.G., Kim, H.J., Min, Y.H., Choi, E.C., Shin, Y.K., Park, B.J., Lee, S.W., and Kim, S. (2005). Human lysyl-tRNA synthetase is secreted to trigger proinflammatory response. Proceedings of the National Academy of Sciences of the United States of America *102*, 6356-6361.
Sato, S., Nomura, F., Kawai, T., Takeuchi, O., Muhlradt, P.F., Takeda, K., and Akira, S. (2000). Synergy and cross-tolerance between toll-like receptor (TLR) 2- and TLR4-mediated signaling pathways. Journal of immunology *165*, 7096-7101.
Seo, H., Hwang, Y., Choe, K., and Kim, P. (2015). In vivo quantitation of injected circulating tumor cells from great saphenous vein based on video-rate confocal microscopy. Biomedical optics express *6*, 2158-2167.
Shen, T., Anderson, S.L., and Rubin, B.Y. (1996). Use of alternative polyadenylation sites in the synthesis of mRNAs encoding the interferon-induced tryptophanyl tRNA synthetase. Gene *179*, 225-229.

Shi, C., and Pamer, E.G. (2011). Monocyte recruitment during infection and inflammation. Nature reviews. Immunology *11*, 762-774.

Shiboski, S.C., Shiboski, C.H., Criswell, L., Baer, A., Challacombe, S., Lanfranchi, H., Schiodt, M., Umehara, H., Vivino, F., Zhao, Y., *et al.* (2012). American College of Rheumatology classification criteria for Sjogren's syndrome: a data-driven, expert consensus approach in the Sjogren's International Collaborative Clinical Alliance cohort. Arthritis care & research *64*, 475-487.

Son, S.H., Park, M.C., and Kim, S. (2014). Extracellular activities of aminoacyl-tRNA synthetases: new mediators for cell-cell communication. Topics in current chemistry *344*, 145-166.

Sonna, L.A., Hawkins, L., Lissauer, M.E., Maldeis, P., Towns, M., Johnson, S.B., Moore, R., Singh, I.S., Cowan, M.J., and Hasday, J.D. (2010). Core temperature correlates with expression of selected stress and immunomodulatory genes in febrile patients with sepsis and noninfectious SIRS. Cell stress & chaperones *15*, 55-66.

Takeuchi, O., Hoshino, K., and Akira, S. (2000). Cutting edge: TLR2-deficient and MyD88-deficient mice are highly susceptible to Staphylococcus aureus infection. Journal of immunology *165*, 5392-5396.

Takeuchi, O., Hoshino, K., Kawai, T., Sanjo, H., Takada, H., Ogawa, T., Takeda, K., and Akira, S. (1999). Differential roles of TLR2 and TLR4 in recognition of gram-negative and gram-positive bacterial cell wall components. Immunity *11*, 443-451.

Vabulas, R.M., Ahmad-Nejad, P., Ghose, S., Kirschning, C.J., Issels, R.D., and Wagner, H. (2002). HSP70 as endogenous stimulus of the Toll/interleukin-1 receptor signal pathway. The Journal of biological chemistry *277*, 15107-15112.

van der Poll, T., and Opal, S.M. (2008). Host-pathogen interactions in sepsis. The Lancet. Infectious diseases *8*, 32-43.

Vitali, C., Bombardieri, S., Jonsson, R., Moutsopoulos, H.M., Alexander, E.L., Carsons, S.E., Daniels, T.E., Fox, P.C., Fox, R.I., Kassan, S.S., *et al.* (2002). Classification criteria for Sjogren's syndrome: a revised version of the European criteria proposed by the American-European Consensus Group. Annals of the

rheumatic diseases *61*, 554-558.
Wakasugi, K., Slike, B.M., Hood, J., Otani, A., Ewalt, K.L., Friedlander, M., Cheresh, D.A., and Schimmel, P. (2002). A human aminoacyl-tRNA synthetase as a regulator of angiogenesis. Proceedings of the National Academy of Sciences of the United States of America *99*, 173-177.
Wang, H., Bloom, O., Zhang, M., Vishnubhakat, J.M., Ombrellino, M., Che, J., Frazier, A., Yang, H., Ivanova, S., Borovikova, L., *et al.* (1999). HMG-1 as a late mediator of endotoxin lethality in mice. Science *285*, 248-251.
Wu, X., Wang, S., Yu, Y., Zhang, J., Sun, Z., Yan, Y., and Zhou, J. (2013). Subcellular proteomic analysis of human host cells infected with H3N2 swine influenza virus. Proteomics *13*, 3309-3326.
Yang, H., Ochani, M., Li, J., Qiang, X., Tanovic, M., Harris, H.E., Susarla, S.M., Ulloa, L., Wang, H., DiRaimo, R., *et al.* (2004). Reversing established sepsis with antagonists of endogenous high-mobility group box 1. Proceedings of the National Academy of Sciences of the United States of America *101*, 296-301.
Yang, H.Y., Kang, K.J., Chung, J.E., and Shim, H. (2009). Construction of a large synthetic human scFv library with six diversified CDRs and high functional diversity. Molecules and cells *27*, 225-235.
Yang, X.L., Otero, F.J., Skene, R.J., McRee, D.E., Schimmel, P., and Ribas de Pouplana, L. (2003). Crystal structures that suggest late development of genetic code components for differentiating aromatic side chains. Proceedings of the National Academy of Sciences of the United States of America *100*, 15376-15380.
Yoon, S.I., Hong, M., and Wilson, I.A. (2011). An unusual dimeric structure and assembly for TLR4 regulator RP105-MD-1. Nature structural & molecular biology *18*, 1028-1035.
Zhou, Q., Kapoor, M., Guo, M., Belani, R., Xu, X., Kiosses, W.B., Hanan, M., Park, C., Armour, E., Do, M.H., *et al.* (2010). Orthogonal use of a human tRNA synthetase active site to achieve multifunctionality. Nature structural & molecular biology *17*, 57-61.
Zhu, H., Cong, J.P., Mamtora, G., Gingeras, T., and Shenk, T. (1998). Cellular gene expression altered by human cytomegalovirus: global monitoring with

oligonucleotide arrays. Proceedings of the National Academy of Sciences of the United States of America *95*, 14470-14475.

국문초록

감염에 대한 초기 면역 방어 시스템에서 Tryptophanyl-tRNA Synthetase 의 역할 규명

Tryptophanyl tRNA synthetase (WRS)는 aminoacyl tRNA synthetases(ARSs)의 일원으로 단백질 합성 과정에 필수적인 효소이다. 최근 이 ARSs들이 본질적인 기능 이외에 다양한 생물학적 기능을 나타낸다는 것이 잘 알려져 있다. 아미노기 부가부분(extra N-terminal domain)이 없는 형태의 mini-WRS는 혈관신생억제 작용을 나타낸다는 것이 보고되었으나 전체 길이의 WRS (full-length WRS; FL-WRS)의 역할에 대해 알려진 바 없었다. 병원체(pathogen)에 의한 것이 아닌 비감염성 원인으로 유발된 각종 전신 염증 반응 (systemic inflammatory response) 환자에서는 WRS의 분비가 증가되지 않는 반면, 박테리아, 바이러스 또는 균류 (fungi)의 감염에 의하여 체내 WRS 수준이 감염 초기부터 빠르게 증가하였다. 특히 패

혈증 환자에서 WRS의 수준이 정상인에 비하여 크게 증가하였다.

본 연구는 병원성 감염원 (세균, 바이러스, 곰팡이 등)이 침입하면 인간의 단핵구로부터 세포질에 존재하던 FL-WRS가 수분 내에 분비되었다. 분비된 FL-WRS는 TLR4-MD2 복합체와 결합하여 대식세포의 식작용을 증가시킴과 동시에 케모카인 분비를 통하여 중성구 (Neutrophil) 유입을 유도함으로서 초기에 감염원을 박멸한다는 것을 밝혔다. 생쥐에 살모넬라균을 감염시키고 FL-WRS를 주입하면 살모넬라균 제거가 활발히 이루어져 생쥐의 생존 기간이 늘어났으며 FL-WRS에 대한 중화 항체를 주입하여 FL-WRS의 작용을 무력화시킨 경우 생쥐의 생존 기간이 줄어드는 것을 확인하였다. 이와 같은 결과는 FL-WRS가 감염 초기에 감염원의 종류에 상관없이 병원균의 침입을 막기 위한 초기 방어 시스템으로 작동한다는 것을 의미한다.

주요어: tryptophanyl-tRNA synthetase (WRS), 패혈증, 감염, 선천면역, TLR4-MD2 복합체

학 번: 2010-30466